The Anti-toxin Properties of Grape Seed Phenolic Compounds

2014

Patrick Cherubin
University of Central Florida

THE ANTI-TOXIN PROPERTIES OF GRAPE SEED PHENOLIC COMPOUNDS

by

PATRICK WALTER CHERUBIN
B.S. University of Central Florida, 2012
A.A. Valencia College, 2010

A thesis submitted in partial fulfillment of the requirements
for the degree of Master of Science
in the Burnett School of Biomedical Sciences
in the College of Medicine
at the University of Central Florida
Orlando, Florida

Summer Term
2014

Major Professor: Kenneth Teter

ABSTRACT

Corynebacterium diphtheriae, Pseudomonas aeruginosa, Ricinus communis, Shigella dysentariae, and *Vibrio cholerae* produce AB toxins which share the same basic structural characteristics: a catalytic A subunit attached to a cell-binding B subunit. All AB toxins have cytosolic targets despite an initial extracellular location. AB toxins use different methods to reach the cytosol and have different effects on the target cell. Broad-spectrum inhibitors against these toxins are therefore hard to develop because they use different surface receptors, entry mechanisms, enzyme activities, and cytosolic targets.

We have found that grape seed extract provides resistance to five different AB toxins: diphtheria toxin (DT), *P. aeruginosa* exotoxin A (ETA), ricin, Shiga toxin, and cholera toxin (CT). To identify individual compounds in grape seed extract that are capable of inhibiting the activities of these AB toxins, we screened twenty common phenolic compounds of grape seed extract for anti-toxin properties. Three compounds inhibited DT, four inhibited ETA, one inhibited ricin, and twelve inhibited CT. Additional studies were performed to determine the mechanism of inhibition against CT. Two compounds inhibited CT binding to the cell surface and even stripped bound CT off the plasma membrane of a target cell. Two other compounds inhibited the enzymatic activity of CT. We have thus identified individual toxin inhibitors from grape seed extract and some of their mechanisms of inhibition against CT. This work will help to formulate a defined mixture of phenolic compounds that could potentially be used as a therapeutic against a broad range of AB toxins.

ACKNOWLEDGMENTS

First and foremost I would like to thank Dr. Ken Teter for allowing me the chance to be part of his team. I was a senior undergraduate when I contacted Dr. Teter about a position in his lab. Dr. Teter invited me to his office, and we discussed about his research. The summer of that same year I applied to an undergraduate research program and I got accepted into the program to work with Dr. Teter on cholera. I have been a research member in Dr. Teter's lab for over three years now, and it has truly been a rewarding experience.

Additionally I would like to thank the rest of my committee members, Dr. Hervé Roy, Dr. Antonis Zervos, and Dr. Otto Phanstiel, for their support and advice throughout the completion of this project. These committee members have "empowered" me throughout the duration of my project. Furthermore I would like to thank Dr. Teter's current and former staff members for all their support and help. When I started working in Dr. Teter's lab, I had no knowledge whatsoever on how to conduct any experiments. The staff members were always there to help me. I want to thank Albert, Aimee, Camila, Carly, Chris, David, Helen, Mike, Neyda, Supriyo, and Tuhina for all their help. Each of these lab mates has contributed in a way or another to my training.

Lastly, I would like to thank the Biotechnology MS program staff members for all their support and academic advice. Ms. Lisa Vaughn, Mr. Eddie Garcia, and Dr. Saleh Naser have been there to assist me ever since I started the program.

Many thanks to each and single one of you!

TABLE OF CONTENTS

LIST OF FIGURES

LIST OF TABLES

LIST OF ACRONYMS

- **AA:** Antibiotic-Antimycotic
- **AC:** Adenylate Cyclase
- **BSA:** Bovine Serum Albumin
- **cAMP:** Cyclic Adenosine Monophosphate
- **CFTR:** Cystic Fibrosis Transmembrane Conductance Regulator Chloride
- **CT:** Cholera Toxin
- **CTA:** Cholera Toxin, A Subunit
- **CTA1:** Cholera Toxin, A1 Subunit
- **CTA2:** Cholera Toxin, A2 Linker
- **CTB:** Cholera Toxin, B Subunit
- **DMEM:** Dulbecco's Modified Eagle Medium
- **DMSO:** Dimethyl Sulfoxide
- **DT:** Diphtheria Toxin
- **DTT:** Dithiothreitol
- **EC_{50}:** Effective Concentration
- **ED_{50}:**Effective Dose
- **EE:** Early Endosomes
- **EDTA:** Ethylenediaminetetraacetic Acid
- **EGCG:** Epigallocatechin Gallate
- **EGFP:** Enhanced Green Fluorescent Protein
- **ER:** Endoplasmic Reticulum

- **ERAD:** ER-associated Degradation
- **ETA:** Exotoxin A
- **FBS:** Fetal Bovine Serum
- **LE:** Late Endosomes
- **NaAc:** Sodium Acetate
- **NAD:** Nicotinamide Adenine Dinucleotide
- **PB1:** Procyanidin B1
- **PB2:** Procyanidin B2
- **PBS:** Phosphate Buffered Saline
- **PDI:** Protein Disulfide Isomerase
- **PKA:** Protein Kinase A
- **RT:** Ricin Toxin
- **RTA:** Ricin Toxin, A Subunit
- **RTB:** Ricin Toxin, B Subunit
- **SDS-PAGE:** Sodium Dodecyl Sulfate Polyacrylamide Gel Electrophoresis
- **ST:** Shiga Toxin
- **STA:** Shiga Toxin, A Subunit
- **STB:** Shiga Toxin, B Subunit
- **TGN:** Trans Golgi Network

CHAPTER 1: INTRODUCTION

Toxins are toxic substances produced by many plants and bacteria. Although there are many different types of toxins, the current study focuses on a subset of AB toxins, a class of toxins containing a catalytic A subunit attached to a cell-binding B subunit. AB toxins are the cause of many diseases. Broad-spectrum inhibitors against AB toxins are hard to develop mainly because different AB toxins use different receptors, entry mechanisms, and targets. The following sub-sections will serve as a brief overview of the different AB toxins that were investigated during the course of this project.

1.1 *Corynebacterium diphtheriae* and Diphtheria Toxin

C. diphtheriae is a Gram-positive bacterium that secretes the AB-type diphtheria toxin (DT) [1]. The C-terminal domain of DT contains the B fragment that is subdivided into two domains, a translocation domain (T) and a receptor binding domain (R) [2]. The catalytic (C) domain of DT is located in the N-terminus of the toxin. Using its R domain, DTB binds to its heparin-binding epidermal growth factor (HB-EGF) receptor on the surface of the cell [1, 3, 4]. DT is then internalized in a clathrin-dependent fashion [5]. The protease furin, which cycles between the cell surface, endosomes, and TGN, cleaves DT between the C and T domain [5, 6]. After furin's cleavage, the C and T domains are still linked via a disulfide bond [5]. In the early endosomes (EE), the acidic environment causes the T domain to undergo a change in conformation during which the hydrophobic regions are inserted into the membrane in order to create a channel through which the C domain translocates to the cytoplasm (Figure 1). In the cytosol, the disulfide bond between the C and T domains gets reduced [7-9]. Following reduction in the cytosol, the C domain ADP-ribosylates elongation factor 2 (eEF-2) by transferring an ADP-ribose group from nicotinamide

dinucleotide (NAD). Following ADP-ribosylation, eEF-2 becomes inactive, subsequently protein translation is halted and programmed cell death occurs [10, 11].

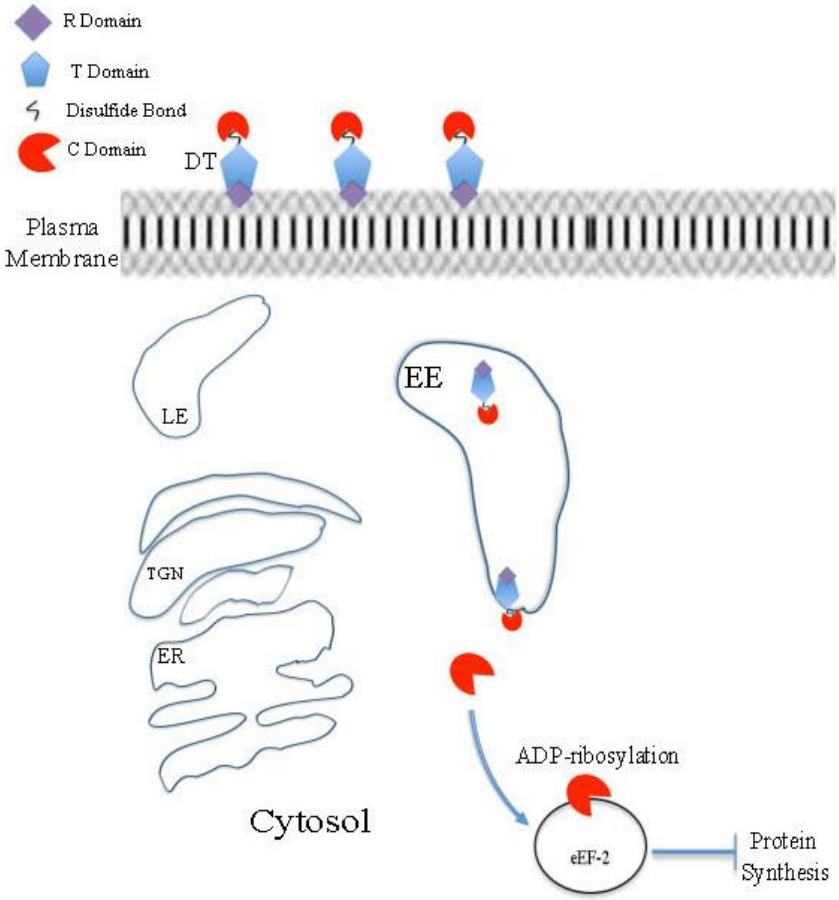

Figure 1: Molecular mechanism of action of DT.

1.2 *Pseudomonas aeruginosa* and Exotoxin A

P. aeruginosa is a Gram-negative bacterium that secretes the virulence factor *Pseudomonas* exotoxin A [12]. ETA is secreted as a multi-domain single polypeptide. The toxin belongs to the AB-type toxin family and it is comprised of three main domains: a receptor binding domain (R or domain I) located in the N-terminus, a translocation domain (T or domain II), and a catalytic domain (C or domain III) [13-15]. The C terminal domain of ETA contains a REDLK peptide sequence from which a secreted host carboxypeptidase removes the lysine (K) residue [16]. Following binding via its R domain to the low-density lipoprotein receptor-related protein (LRP) [17, 18], ETA gets internalized via endocytic vesicles and clathrin-coated pits [19]. ETA is then cleaved by furin protease in a furin-sensitive loop located in the T domain [6, 20-22]. Following cleavage by furin, the C and T domains remain linked by a disulfide bond. Reduction of the disulfide bond by PDI or PDI-like enzyme partially separates the catalytic C domain from the T domain, allowing the C domain to migrate to the TGN aided by Rab9 [23, 24]. A part of the T domain still remains bound to the C domain [23, 24]. In the Golgi, the REDL sequence located at the toxin C-terminus binds to KDEL intracellular sorting receptor, allowing its transport to the ER. In the ER, part of the T domain still bound to the C domain via a disulfide bond helps translocate the C domain to the cytoplasm [16, 25, 26]. In the cytosol, the C domain ADP-ribosylates eEF-2, thereby inactivating it (Figure 2). Inactivation of eEF-2 ultimately leads to inhibition of protein synthesis and programmed cell death [27].

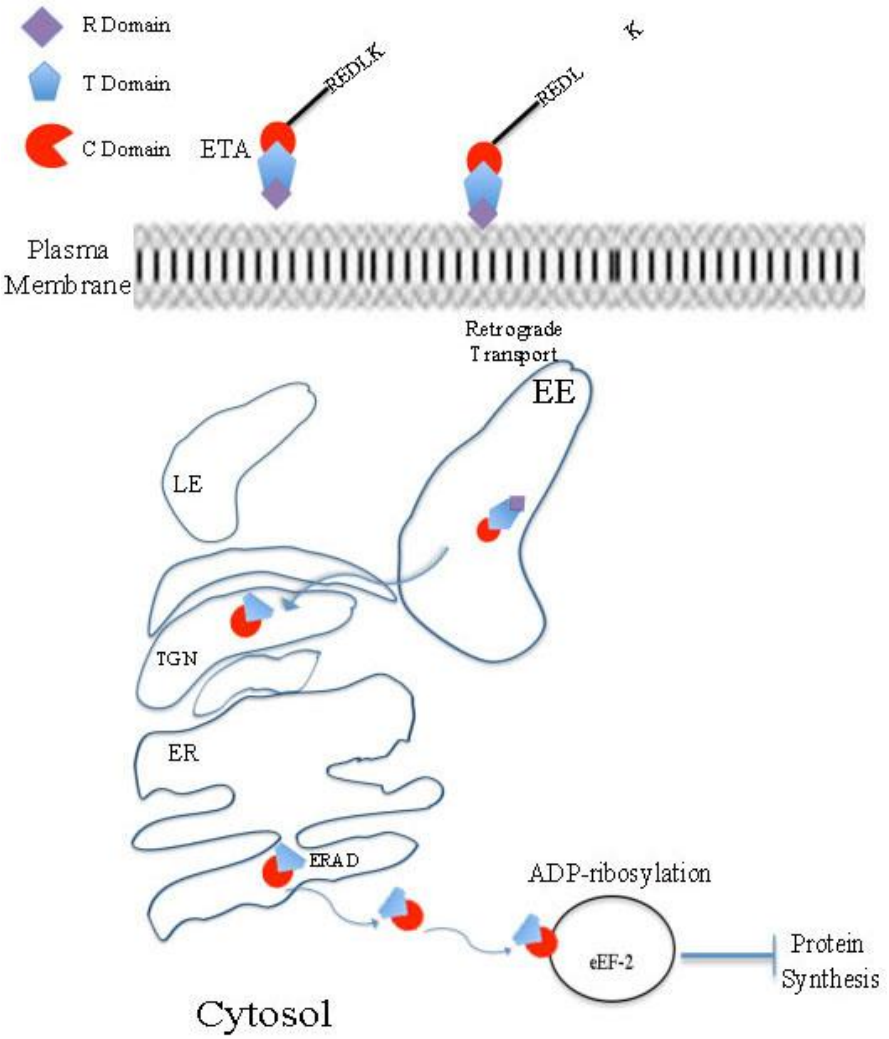

Figure 2: Molecular mechanism of action of ETA.

1.3 *Ricinus communis* and Ricin Toxin

Castor bean from the *R. communis* plant produces ricin toxin as a natural by-product. Ricin is a type II ribosome inactivating protein (RIP II). Bacteria and, most commonly, plants produce RIPs. In fact, RIPs have originally been known as an antiviral agent that certain plants like pokeweed uses [28, 29]. There are several reports of the use of ricin in biological warfare [30]. Ricin is a category B biothreat agent. Currently there are no known countermeasures against ricin [31, 32]. Ricin is a single chain AB-type toxin composed of an A subunit linked to a B subunit via a disulfide bond. Ricin binds to galactose or N-acetylgalactolamine residues located on glycoproteins and glycolipids using its lectin B subunit [33, 34]. Following clathrin-dependent or clathrin-independent endocytosis, ricin gets retrotransported from the EE to the Golgi, and then to the ER (Figure 3) where its disulfide bond gets reduced [35, 36]. Using the ERAD quality control process, the A subunit of ricin enters the cytosol via the sec61p translocon [37-39]. In the cytosol, the A subunit of ricin attacks the ribosome by removing a specific adenine residue (Depurination) from the 28S rRNA loop known as the "sarcin/ricin loop". Removal of this adenine residue disrupts the interaction between the ribosome and eEF-2, causing translation inhibition and ultimately cell death by apoptosis [40-42]. Also, many studies are being conducted to investigate potential anti-cancer uses of ricin. Since it causes cell death, scientists are investigating its use in gene therapy and immunotoxins to selectively target cancer cells [43].

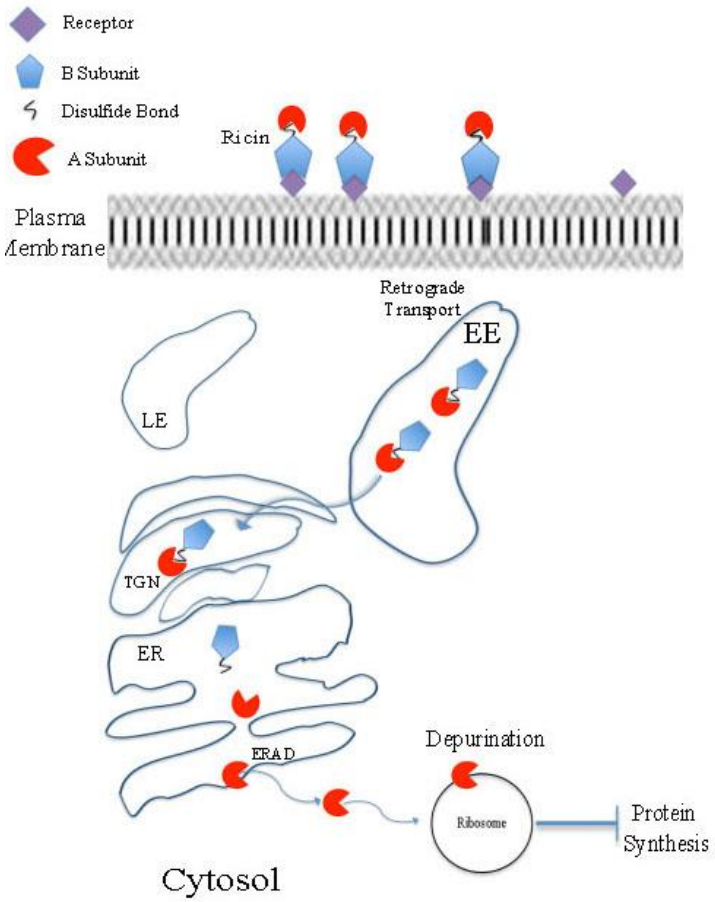

Figure 3: Molecular mechanism of action of ricin.

1.4 *Shigella dysentariae* and Shiga Toxin

S. dysentariae type 1 is a Gram-negative bacterium that secretes Shiga toxin (ST) as a virulence factor. *S. dysentariae*, isolated by Dr. Kiyoshi Shiga in 1896, was the first known species of *Shigella* [44-46]. Other types of bacteria such as enterohemorrhagic *Escherichia coli* (EHEC) also produce Shiga-like toxins [47]. Shiga toxins are involved in several diseases including dysentery, Shigellosis, hemolytic uremic syndrome [48], and others [44, 46, 49, 50]. ST belongs to the family of AB toxins and it has a B binding (STB) subunit and a catalytic A (STA) subunit. STA1 is connected to STA2 by a disulfide bond just like CT [51, 52]. ST has the same AB_5 organization as CT. There are different groups of STs depending on the organism producing the toxin [50, 53]. ST trafficking involves STB binding to membrane glycolipid Gb_3, from which it is endocytosed through clathrin coats. Furin cleaves STA in the endosomes and/or TGN to generate a disulfide-linked STA1/STA2 heterodimer. Reduction of the STA1/STA2 disulfide bond in the ER allows STA1 to dissociate from STA2 before entering the cytosol [47, 54-56]. In the cytosol, STA1 irreversibly inactivates the ribosome by the removal of an adenine residue (Depurination) from the 28S rRNA of the larger 60S ribosomal subunit (Figure 4), thereby inhibiting protein translation and causing cell death [57, 58].

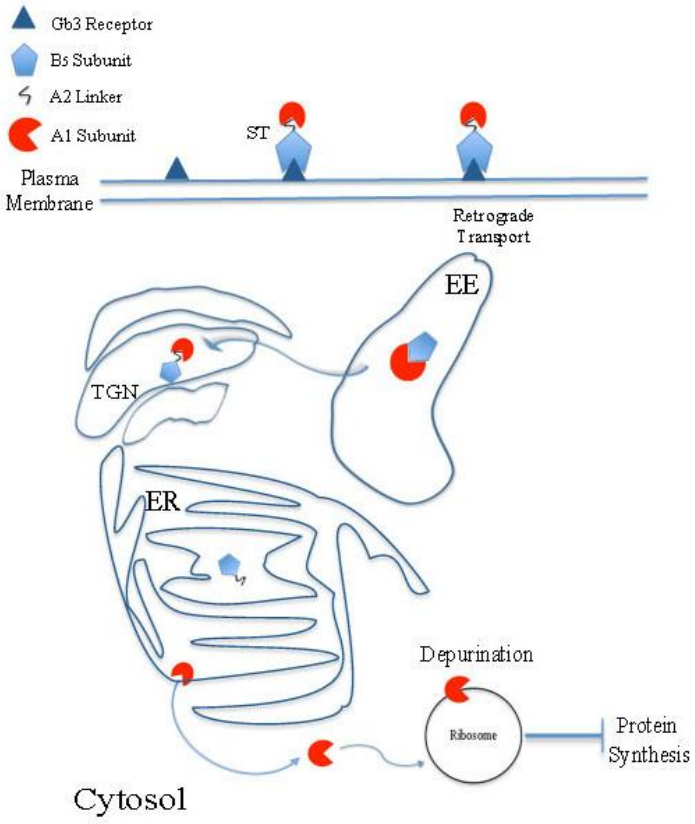

Figure 4: Molecular mechanism of action of ST.

1.5 *Vibrio cholerae* and cholera toxin

V. cholerae is a Gram-negative bacterium that causes cholera, a significant water-borne diarrheal disease. While water is usually considered to be the main route of *V. cholera* transmission, it can also be transmitted through contaminated food. Cholera is very rare in industrialized countries, mainly because of good sanitation. The last major cholera outbreak was the case of Haiti in 2010 [59]. The main symptom of cholera is water and electrolyte loss caused by the diarrhea. If not treated, cholera can lead to death. Oral rehydration solutions to replace the loss of fluids and electrolytes are the main treatment for cholera. Antibiotics are often used as a supplement that helps reduce the duration and severity of the disease. However, due to the rise of antibiotic-resistant *V. cholerae* strains, new low-cost therapies that also reduce the duration and severity of the disease are needed as an alternative to antibiotics.

Cholera toxin (CT) is the main virulence factor released from *V. cholerae* [60, 61]. CT is an AB-type toxin that is released into the lumen of the gut and activates by ADP-ribosylation Gsα, the stimulatory subunit of the heterotrimeric G protein needed to activate adenylate cyclase and the cAMP signaling pathway [62-64]. The A subunit of CT is a single polypeptide that can be converted by proteolysis to a disulfide-linked heterodimer consisting of a catalytic CTA1 moiety and a CTA2 fragment which links CTA1 to the CTB binding domain. The B subunit of CT is a pentameric ring-like structure that binds to GM1 gangliosides on the eukaryotic plasma membrane (Figure 5). Once bound to the cell surface, CT is endocytosed and delivered to the endoplasmic reticulum (ER) through the trans-Golgi network (TGN) by retrograde vesicular transport [60, 62]. Reduction of the CTA1/CTA2 disulfide bond occurs in the (ER) [65, 66], and subsequently allows protein disulfide isomerase (PDI) to release the CTA1 polypeptide from the rest of the toxin [67, 68]. CTA1 then unfolds, which facilitates its entry to the cytosol by the quality control mechanism

of ER-associated degradation (ERAD) [69-72]. Cytosolic CTA1 then initiates the intoxication process by ADP-ribosylation of Gsα. The constitutive activation of adenylate cyclase by Gsα leads to an increased level of cAMP. High levels of cAMP cause the activation of protein kinase A (PKA), which ultimately leads to the phosphorylation of the cystic fibrosis transmembrane conductance regulator chloride (CFTR) channel [62, 73-75]. CFTR phosphorylation causes the channel to open, thereby releasing chloride ions in the intestinal milieu. The release of the chloride ions, accompanied with water, is what causes the diarrhea response of the cholera disease.

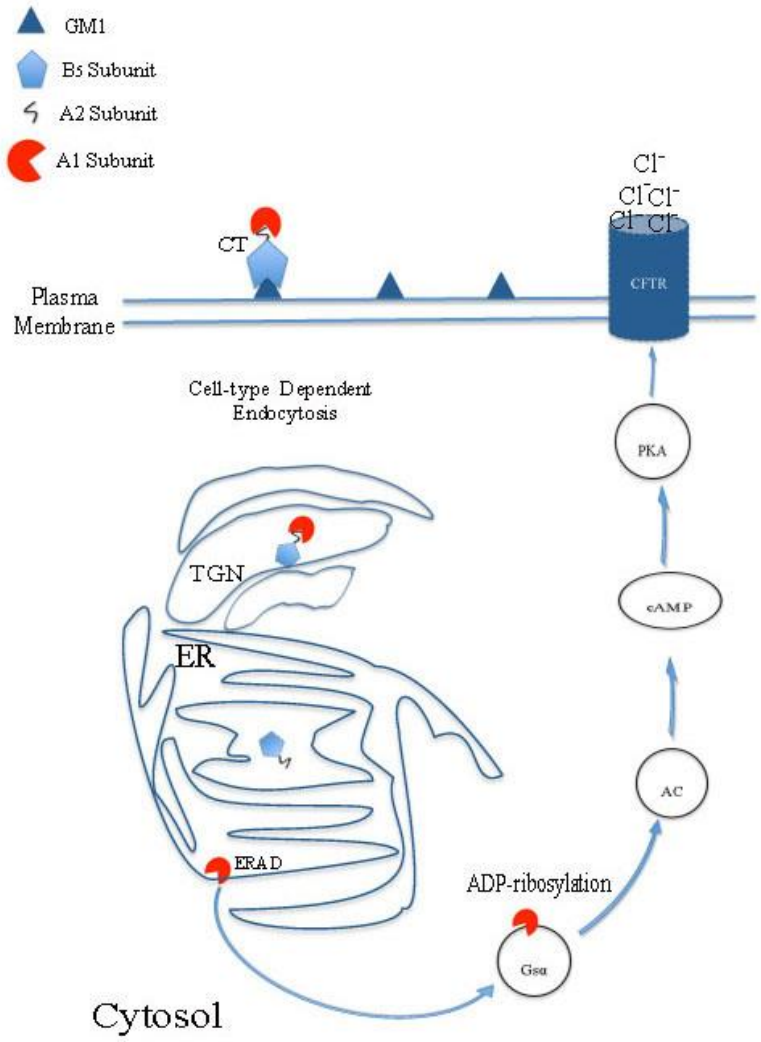

Figure 5: Retrograde trafficking of CT.

1.6 Hypothesis and Aims

All the toxins discussed above share an AB structural organization. All these toxins are endocytosed from the plasma membrane and reach the cytosol from an intracellular organelle (Table 1). DT, from *C. diphtheriae*, moves from an acidified endosome to the cytosol where it modifies eEF-2 by ADP-ribosylation. This causes an inhibition of protein synthesis in the host cell. ETA, from *P. aeruginosa*, moves from the ER to the cytosol to inhibit protein synthesis by ADP-ribosylation of eEF-2. CT, from *V. cholerae*, RT from *R. communis*, and ST from *S. dysentariae* enter the cytosol from the ER. RT and ST both inhibit protein synthesis by the removal of a specific adenine residue in the 28S rRNA of the large 60S ribosomal subunit, thereby rendering the ribosome unable to interact with eEF-2. CT, on the other hand, targets cytosolic Gsα. Despite their structural similarities, these toxins each have different surface receptors, different intracellular trafficking mechanisms, and different cytosolic targets. Thus, formulating broad-spectrum inhibitors for these toxins is difficult.

In many cultures, herbal remedies have been used for centuries to help alleviate diarrheal diseases like cholera [76, 77]. Dietary consumption of grape products, red wine in particular, has been shown to be associated with lower incidence of cardiovascular disease and certain types of cancer. Grape extract possesses many relevant biological activities, such as antioxidant and antimicrobial properties [78, 79]. Recently, the Teter lab has shown that grape seed extract confers resistance against CT [80]. Grape seed extract has also been identified to confer resistance against ST [81]. Because grape seed extract is rich in phenolic compounds [82-84] (Figure 6), we hypothesized that one or more phenolic compounds from grape extract are responsible for generating resistance to CT and ST. The present work primarily aimed to identify the specific phenolic compounds in the extract that are responsible for CT inhibition and to determine the

mechanism of inhibition. Another aim of this project was to identify a broad-spectrum inhibition of the phenolic compounds against other AB-type toxins. The use of antibiotics against bacterial infection causes a problem because of the selective pressure that they exert on the pathogens that can give rise to resistant strains. Therefore new approaches are in need to help fight bacterial pathogens. Natural compound usage against CT, from *V. cholerae*, is a good approach because, unlike antibiotics, it will be less likely to induce a selective pressure on the bacterial pathogens that can lead to resistance because it does not directly affect the growth or viability of the pathogen. Therefore the present work can be used as a foundation for the synthesis of broad-spectrum therapeutic agents against cholera and other toxin-mediated diseases.

Table 1: Toxins comparison chart.

Toxin	Receptor	Endocytosis	Translocation Site	Cytosolic Target	Action on Target
DT	HB-EGF	Clathrin-dependent	Acidified Endosomes	eEF-2	ADP-ribosylation
ETA	LRP	Clathrin-dependent	ER	eEF-2	ADP-ribosylation
Ricin	Glycoproteins/lipids with terminal galactose	Clathrin-dependent and clathrin-independent	ER	28S rRNA of the 60S ribosome	Depurination
ST	Gb_3 glycolipid	Clathrin-dependent	ER	28S rRNA of the 60S ribosome	Depurination
CT	GM1	Clathrin-independent	ER	Gsα	ADP-ribosylation

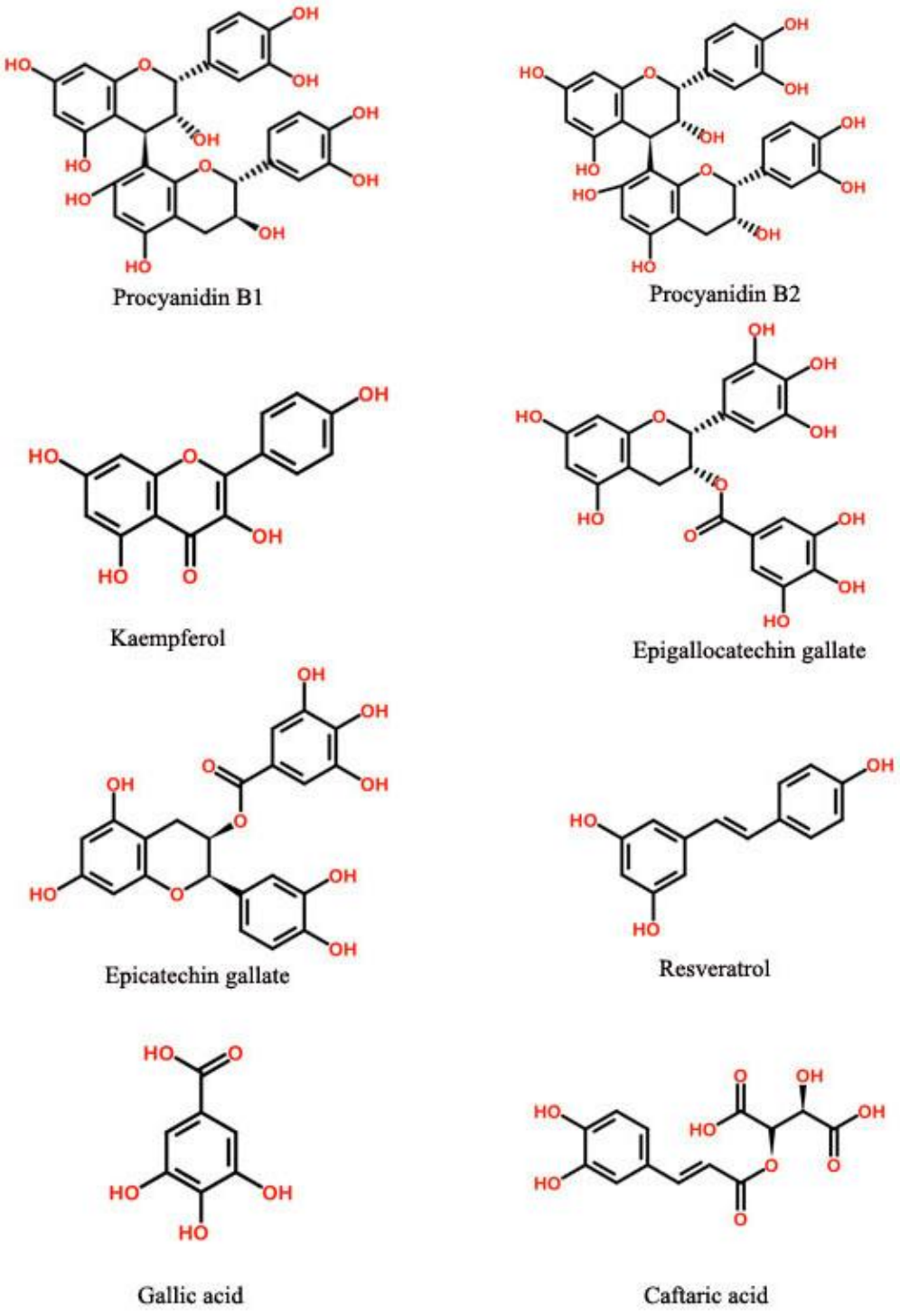

Figure 6: The chemical structures of 8 phenolic compounds.

CHAPTER 2: MATERIALS AND METHODS

2.1 Chemicals and Reagents

Amresco (Solon, OH)

- 4-(2-hydroxyethyl)-1-piperazineethanesulfonic acid (HEPES)
- Ammonium persulfate (APS)
- Bromophenol blue
- Glacial acetic acid
- Glycine
- Sodium dodecyl sulfate (SDS)
- Tris-Cl

Atlanta Biologicals (Lawrenceville, GA)

- Fetal bovine serum (FBS)

Bio Rad (Hercules, CA)

- 40% Acrylamide/Bis solution
- AG 50W-X4 ion exchange resin beads

Fisher Scientific (Pittsburgh, PA)

- 200 proof ethanol (EtOH)
- 2-mercaptoethanol (β-ME)
- 4-diethylaminobenzaldehyde
- Bovine serum albumin (BSA)
- CellTiter 96 AQueous One solution cell proliferation assay (MTS)
- Dimethyl sulfoxide (DMSO)

- Forskolin *Coleus forskohlii*
- Gel code blue stain reagent
- Glycerol
- Methanol (MeOH)
- Phosphate monobasic monohydrate ($Na_2HPO_4H_2O$) tris base
- Slide-A-lyzer mini dialysis units (3500 MWCO)
- Sodium chloride (NaCl)
- Sodium hydroxide (NaOH)
- Sodium phosphate dibasic anhydrous (Na_2HPO_4)
- Sodium phosphate dibasic heptahydrate ($Na_2HPO_4 \cdot 7H_2O$)
- Sodium phosphate monobasic anhydrous (NaH_2PO_4)

GE Healthcare (Piscataway, NJ)

- ELISA cAMP kit

Gibco (Grand Island, NY)

- Antibiotic-antimycotic (AA)
- Dulbecco's modified eagle medium (DMEM)

Invitrogen (Carlsbad, CA)

- Antibiotic-antimycotic (AA)
- Dulbecco's modified eagle medium (DMEM)
- Ham's F-12
- SilverQuest staining kit
- Trypsin/EDTA

Mediatech, Inc. (Manassas, VA)

- Phosphate-Buffered Saline, 1X

Pierce Biotechnology, Inc. (Rockford, IL)

- BCA protein assay kit

Santa Cruz Biotechnology, Inc.

- 4-Diethylaminobenzaldehyde
- Aminoguanidine bicarbonate

Sigma Aldrich (St. Louis, MO)

- α-Casein from bovine milk
- 200 proof ethanol (EtOH)
- Aminoguanidine bicarbonate
- Ethylenediaminetetraacetic acid (EDTA)
- Glycerol
- Sodium phosphate dibasic heptahydrate ($Na_2HPO_4 \cdot 7H_2O$)
- Tetramethylethylenediamine (TEMED)
- Thermolysin from *Bacillus thermoproteolyticus*
- Trypan blue solution

2.2 Plant Extracts and Phenolic Compounds (with Stock Concentration and Solvent)

Chromadex, Inc. (Irvine, CA)

- Caftaric acid (2.5 mg/ml in H_2O)
- Cyanidin-3-diglucoside (1 mg/ml in H_2O)
- Delphinidin-3-O-glucoside (2.5 mg/ml in H_2O)
- Gallic acid (2.5 mg/ml in H_2O)

- Grape (*Vitis vinifera*) seed XRM (10 mg/ml in H_2O)
- Kuromanin chloride (2.5 mg/ml in H_2O)
- Peonidin-3-glucoside chloride (2.5 mg/ml in H_2O)
- Petunidin-3-glucoside chloride (2.5 mg/ml in H_2O)
- Procyanidin B1 (2.5 mg/ml in H_2O)
- (+)-Procyanidin B2 (2.5 mg/ml in H_2O)
- Protocatechin (2.5 mg/ml in H_2O)
- Quercitrin (1 mg/ml in EtOH)

Extrasynthese (Genay Cedex, France)

- Kaempferol-3-Glucoside (2.5 mg/ml in MeOH)
- Malvin chloride (2.5 mg/ml in MeOH + 0.1% HCl)
- Oenin chloride (2.5 mg/ml in MeOH + 0.1% HCl)

Polyphenolics, Inc. (Madera, CA)

- Gold grape seed extract (10 mg/ml in H_2O)

Sigma Aldrich (St. Louis, MO)

- (-)-Catechin (2.5 mg/ml in H_2O)
- (-)-Catechin gallate (2.5 mg/ml in H_2O)
- (-)-Epicatechin (2.5 mg/ml in H_2O)
- (-)-Epicatechin gallate from green tea (2.5 mg/ml in H_2O)
- (-)-Epigallocatechin gallate (2.5 mg/ml in H_2O)
- Resveratrol (2.5 mg/ml in EtOH)

2.3 Buffers

4X SDS-PAGE Sample Loading Buffer

- 0.04% bromophenol blue
- 0.1 M 2-mercaptoethanol (ß-ME)
- 0.24 M tris-HCl, pH 6.8
- 40% glycerol
- 8% SDS

10X Phosphate Buffered Saline (PBS)

- 0.69 M NaCl
- 0.17 M NaH_2PO_4
- 0.58 M Na_2HPO_4

10X SDS-PAGE Running Buffer

- 0.025 M tris base
- 0.1% SDS
- 0.192 M glycine

2.4 Toxins

List Biological Laboratories (Campbell, CA)

- Cholera toxin, A subunit
- Cholera toxin, holotoxin
- Diphtheria toxin
- Exotoxin A from *Pseudomonas aeruginosa*
- Shiga toxin 2

Sigma Aldrich (St. Louis, MO)

- Cholera holotoxin
- Cholera toxin A subunit
- Fluorescein isothiocyanate-conjugated CTB pentamer (FITC-CTB)

Vector Laboratories (Burlingame, CA)

- *Ricinus communis* agglutinin II

2.5 Equipments

Bio Rad (Hercules, CA)

- Bio Rad PowerPac Basic
- Bio Rad PowerPac HC
- Gel Doc 2000

BioTek Instruments (Winooski, VT)

- Synergy 2 plate reader

2.6 Cell Lines

- Chinese hamster ovary (CHO) cells
- Vero cells
- Vero-d2EGFP cells

2.7 Data Processing Softwares

- Adobe photoshop
- KaleidaGraph
- Microsoft excel

2.8 Other Materials

VWR International (Aurora, CO)

- 10 cm tissue culture dish
- 24-well tissue culture plate
- 6-well tissue culture plate
- Cellstar, 96-well cell culture plate
- Costar assay plate, 96-well black-walled with clear flat bottom
- Fisher scientific hemocytometer

2.9 Techniques

Cell Culture

All cells were split when they reached about 80% confluency. This confluency was usually reached every 3 to 4 days for the cells used. Cells in a 10 cm dish were washed once with phosphate buffered saline (PBS). Following the PBS wash, 1 ml of trypsin-EDTA was added for about 5 minutes in order to lift the cells from the dish. For CHO cells, 9 mls of Ham's F-12 medium containing 10% FBS and 1% AA was added to resuspend the cells. For Vero and Vero-d2EGFP cells, 9 mls of Dulbecco's Modified Eagle Medium (DMEM) containing 10% FBS and 1% AA was added to resuspend the cells. For each new 10 cm dish, 9 mls of the appropriate medium and 1 ml of cell resuspension were added. Evenly distributed cells in the 10 cm dish were then placed in a 37ºC incubator under 5% CO_2. For the 96-well plate, a 1:10 dilution of the 10 ml cell suspension was used to seed the plate (100 µl per well). For the 24-well plates, a 1:5 dilution of the 10 ml cell suspension was used to seed the plate (500 µl per well for the 24 well-plates). 80% confluency was reached within 18 to 24 hours prior to intoxication.

cAMP Toxicity Assay

Flat bottom 24-well plates were used to seed CHO cells in triplicate. The cells reached 80% confluency after an overnight incubation. After one wash with PBS, Ham's F-12 serum-free medium with various dilutions of CT in the presence or absence of treatments was added to the plate. After incubation the cells were washed again with PBS. 15 minute incubation with 0.25 ml of ice cold HCl: EtOH (1:100) at 4ºC was used to lyse the cells. The cell extracts were transferred to new 24-well plates and allowed to air dry overnight. Following reconstitution in assay buffer, the levels of cAMP were determined by using the ELISA cAMP competition assay kit as described by the manufacturer. Unintoxicated cells were used to establish the background level of cAMP. The background level was subtracted from each cAMP value, and these values were expressed as percentages of the maximum response from untreated CHO cells, which was arbitrarily set as the 100% value.

Measurement of Cell Viability with the MTS Assay

To monitor cell viability in the presence of phenolic compounds, CHO cells were seeded in a 96-well plate and allowed to reach ~80% confluency overnight at 37ºC under 5% CO_2. The next day, cells were treated in the presence or absence of 10 μg/ml dilution of the specified phenolic compounds in serum-free F-12 medium for an additional overnight incubation at 37ºC. The day after, 20 μl of a commercially available MTS reagent was added to each well of the plate for a 3 hour incubation at 37ºC. NADPH and NADH from live, metabolically active cells reduce the MTS reagent into a colored formazan product that can be detected at an absorbance of 490 nm using a Synergy 2 plate reader. The formazan absorbance at 490 nm is directly proportional to the extent of cell viability.

Toxin Binding Assay

Vero cells grown to 80% confluency in 96-well clear-bottom black-walled plates were treated with 100 μl of 1 μg/ml dilution of FITC-CTB in serum-free DMEM media at 4°C in the presence or absence of drug treatments for 1 hour. Following the incubation, the cells were washed with PBS. A Synergy 2 plate reader was used to measure the fluorescence intensity using 485/20 nm excitation and 528/20 nm emission wavelength filters. A set of untreated Vero cells was used as the background fluorescence level and was subtracted from each value. To investigate whether or not the grape seed extract, PB2 or EGCG could strip bound FITC-CTB off the cell surface, the FITC-CTB was allowed to bind to the cell surface for 30 minutes at 4°C before the addition of the individual treatment conditions. For the dialysis experiment, a 3.5 kD mini dialysis cup was used. Specific conditions were added to the dialysis cup and allowed to dialyze overnight in PBS (pH 7.4). The next day the contents of the dialysis cup were added to Vero cells for 1 hour at 4°C followed by PBS washes before the fluorescence intensity measurement.

In Vitro CTA1 Activity Assay

To monitor the ADP-ribosyltransferase activity of CTA1, aminoguanidine bicarbonate and 4-diethylaminobenzaldehyde were used to synthesize diethylamino(benzylidine-amino)guanidine (DEA-BAG), a substrate for ADP-ribosylation [85]. DEA-BAG was synthesized by making a 0.11 M solution of aminoguanidine bicarbonate, pH 6.5. After filtration to remove insoluble solids, the solution was heated to 60°C. 4-Diethylaminobenzaldehyde in 200 proof EtOH was added to the filtrate in a 1:1 molar ratio with the aminoguanidine bicarbonate (Figure 7). The solution was allowed to stir at room temperature overnight, and the precipitated DEA-BAG was harvested by filtration, lyophilized, and placed at -80°C for long-term storage.

Specified conditions of CTA samples were diluted in 0.2 M KH_2PO_4, pH 7.5 with 0.02 M DTT, 0.1 mg/ml BSA, 0.01 M NAD, and 0.02 M DEA-BAG. After a 2 hour incubation at room

temperature, AG 50W-X4 ion exchange resin beads was added to the reaction. Unmodified DEA-BAG binds to the resin beads, whereas ADP-ribosylated DEA-BAG does not. A tabletop centrifuge was used to spin the samples at maximum speed for 15 minutes. The supernatant from the samples were used to measure the extent of ADP-ribosylation of DEA-BAG (Figure 8). The intrinsic fluorescence of DEA-BAG was measured using a Synergy 2 plate reader at 360 nm excitation and 460 nm emission wavelengths. A set of DEA-BAG with no CTA treatment was used as the background fluorescence level and was subtracted from each value.

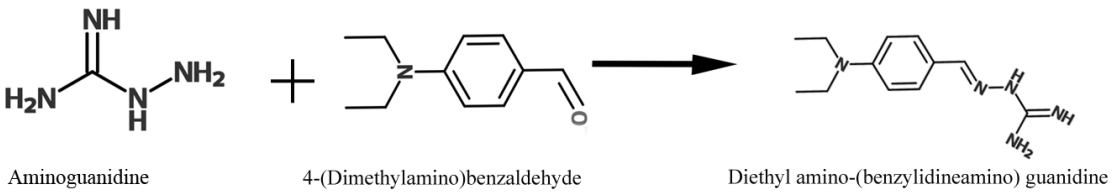

Aminoguanidine 4-(Dimethylamino)benzaldehyde Diethyl amino-(benzylidineamino) guanidine

Figure 7: The synthesis of DEA-BAG.

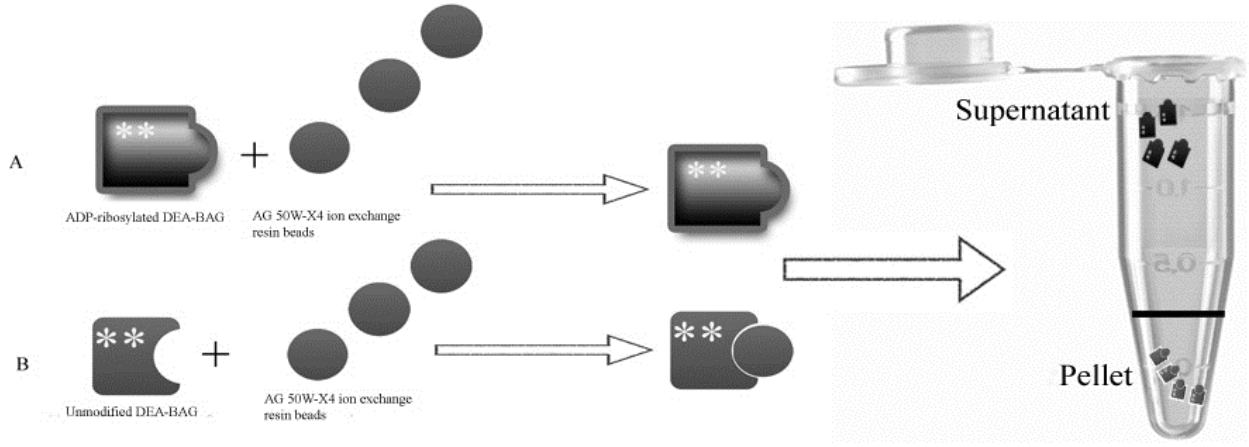

Figure 8: In vitro DEA-BAG assay.

A) When DEA-BAG is ADP-ribosylated by CTA1 it is unable to bind the resin beads and remains in the supernatant following application of a centrifugal force.

B) Unmodified fluorescent DEA-BAG binds the resin beads and migrates to the bottom of the tube when a centrifugal force is applied.

The fluorescent intensity of the supernatant is thus directly related to the extent of toxin activity.

Protease Sensitivity Assay

The thermolysin assay is used to monitor the folding state of CTA1 (Figure 9). The basis behind this assay is that an unfolded protein is less resistant to protease activities than a folded protein. Upon addition of the thermolysin protease to the samples, unfolded CTA1 will be degraded and no band will be present when resolved on a gel, whereas folded CTA1 is more resistant to proteolysis and shows up as a band on a gel.

A 20 mM $NaPO_4$ buffer (pH 7.4) with 10 mM β-ME was used to reduce the 1 μg CTA samples. The samples (20 μl) were then incubated under specified temperatures for an hour. After the 1 hour incubation the samples were allowed to equilibrate at 4°C for 10 minutes. Following the 4°C equilibration, the protease reaction was conducted by adding 2 μl from a 0.4 mg/ml thermolysin protease solution in 0.05 M $CaCl_2$ and 0.1 M HEPES (pH 8.0) to the samples for an additional 1 hour 4°C incubation. To halt the protease reaction, 3 μl of a 0.1 M EDTA was added to the samples for 5 minutes 4°C incubation. After adding 5 μl from a 4X SDS-PAGE loading buffer to the samples, the samples were boiled for 5 minutes. Following boiling, 25 μl from the 30 μl total final volume was resolved using a 12% SDS-PAGE gel, and Coomassie staining was used for visualization.

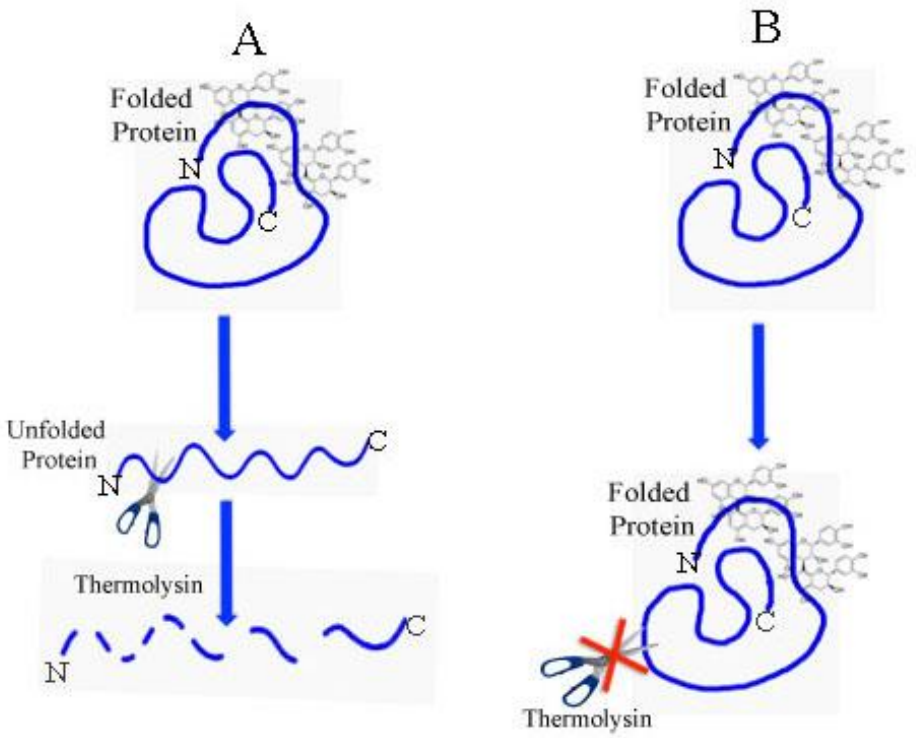

Figure 9: Thermolysin assay for CTA1 unfolding.

Panel A: Phenolic compounds that do not inhibit CTA1 unfolding at 37°C will not protect CTA1 from thermolysin.

Panel B: Phenolic compounds that inhibit CTA1 unfolding at 37°C will protect CTA1 from thermolysin.

Vero-d2EGFP Assay

The Vero-d2EGFP assay is a fluorescence-based toxicity assay that was used to monitor protein synthesis in the presence of DT, ETA, ricin, and ST. As described by Quiñones et al. [81], the Vero-d2EGFP cells were seeded in a 96-well black-walled plate with clear flat bottom and incubated overnight in a 37°C humidified incubator under 5% CO_2. The next day, the cells reached ~ 80% confluency. After a PBS wash, the cells were treated with specific toxins diluted in serum-free Ham's F-12 medium. After an additional overnight incubation at 37°C, the cells were washed three times with PBS. Following the PBS washes, a Synergy 2 plate reader with the 485/20 nm excitation filter and the 528/20 nm emission filter was used to measure EGFP fluorescence level. The fluorescence level of EGFP was expected to be inversely proportional to the activity of the toxins (Figure 10). A set of unintoxicated parental Vero cells was used as the background EGFP signal and was subtracted from each value. The values are expressed as a percentage of the maximum fluorescent signal from Vero-d2EGFP cells incubated in the absence of toxin, which was set as the 100% value.

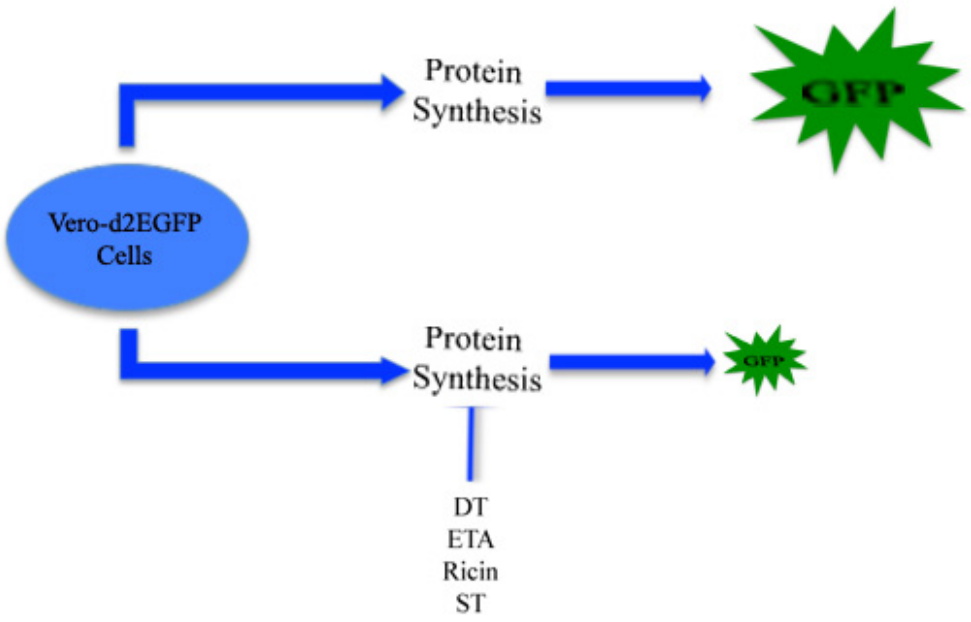

Figure 10: Vero-d2EGFP to monitor protein synthesis activity.

CHAPTER 3: RESULTS

Quiñones et al. have reported that grape seed extract can reduce the activity of ST in cultured cells [81]. Therefore the Vero-d2EGFP assay was used to further investigate the anti-toxin properties of grape seed extract against other AB toxins, namely DT, ETA and ricin. The cell line used here expresses a variant of GFP with a 2 hour half-life. The toxins under study block protein synthesis, so there is an inverse correlation between toxin activities and the GFP signal. An increase in the toxins' activity will result in lower GFP signal, and vice versa. Unintoxicated Vero-d2EGFP cells are arbitrarily set as the 100% maximal EGFP signal value, and all the individual values are expressed as a ratio of that maximal EGFP signal. A 100 μg/ml grape seed extract concentration was used to investigate the anti-toxin property of the grape seed extract against each of these toxins. This is the same concentration used in the Quiñones et al. paper.

3.1 Grape Seed Extract Inhibits the Activity of DT, ETA and Ricin

Using the Vero-d2EGFP assay, we intoxicated the cells with DT to generate a dose-response curve. The EC_{50} was determined to be ~0.01 ng/ml (Figure 11). When the cells were intoxicated along with a 100 μg/ml grape seed extract concentration, the activity of DT was significantly reduced. An ED_{50} could not be calculated for DT intoxication in the presence of grape seed extract. When compared to nearly a complete loss of fluorescence signal for DT alone at 0.1 ng/ml, the fluorescence signal was still ~90% of the untreated signal. This suggests a high resistance to DT.

A dose-response curve was generated for Vero-d2EGFP cells treated with ETA. The EC_{50} of ETA was ~35 ng/ml (Figure 12). ETA-intoxicated cells treated with a 100 μg/ml concentration of grape seed extract showed a higher level of protein synthesis compared to untreated cell samples,

with about 75% of the untreated fluorescent signal remaining in Vero-d2EGFP cells exposed to the highest ETA concentration of 100 ng/ml.

A dose-response curve was generated for Vero-d2EGFP cells treated with ricin. The EC_{50} of ricin was found to be ~0.05 ng/ml (Figure 13). When the cells intoxicated with ricin were treated with grape seed extract, a higher level of protein synthesis was detected. About 60% of the untreated fluorescence signal was detected in Vero-d2EGFP cells exposed to both 1 ng/ml ricin and grape extract, compared to a nearly complete loss of protein fluorescence signal in cells exposed to 1 ng/ml of ricin alone.

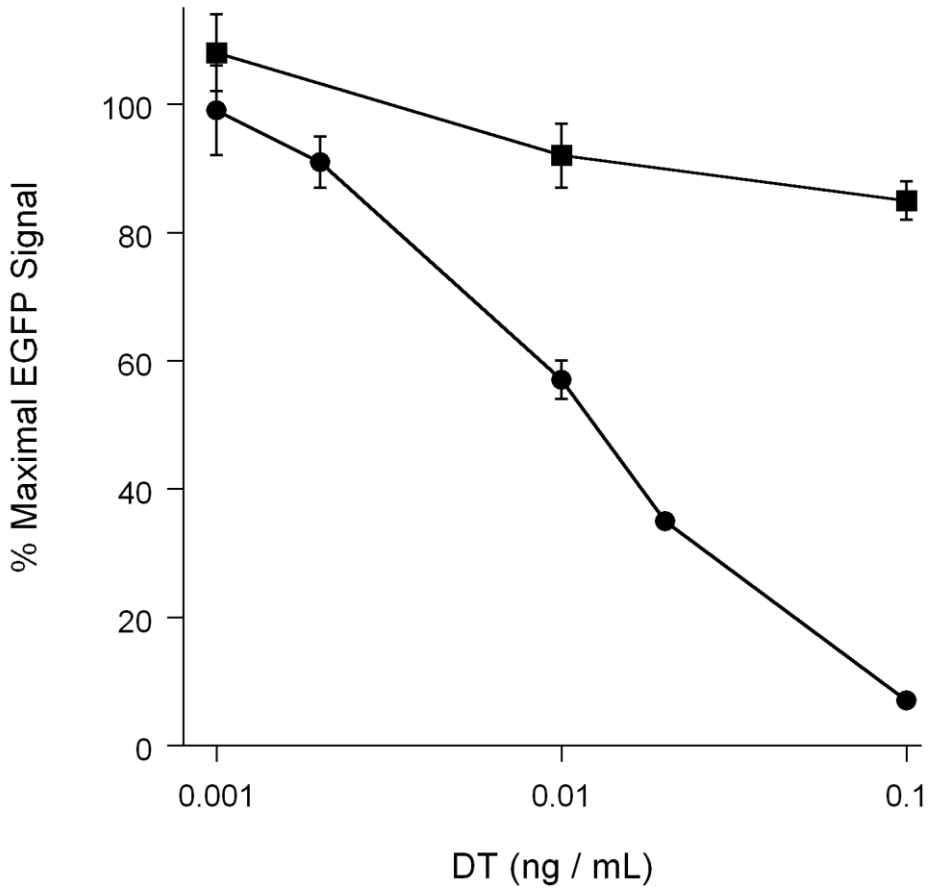

Figure 11: The effect of DT on Vero-d2EGFP signal.

EGFP signal was measured after an overnight incubation with the indicated concentrations of DT. Error bar represents the means of 3-5 independent experiments with 6 or 12 replicate samples for each condition. The circle denotes Vero-d2EGFP samples intoxicated with DT only, and the square denotes the co-incubation of DT with grape seed extract.

The EGFP signal from untreated Vero-d2EGFP cells was arbitrarily set as the 100% maximal EGFP signal.

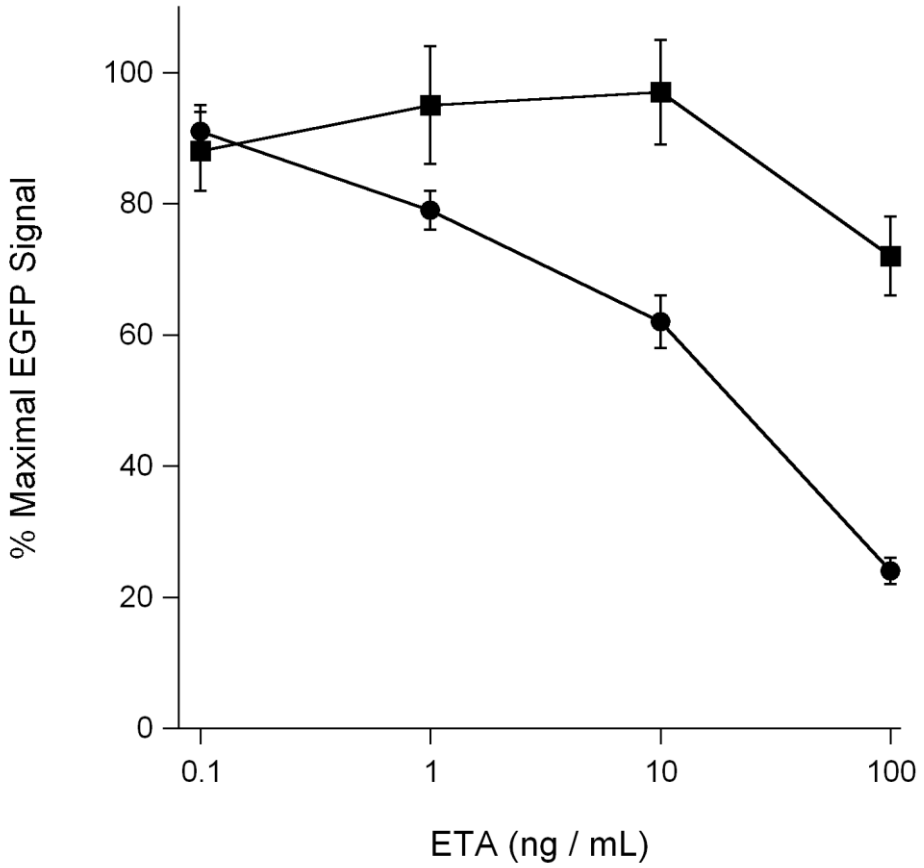

Figure 12: The effect of ETA on Vero-d2EGFP signal.

EGFP signal was measured after an overnight incubation with the indicated concentrations of ETA. Error bar represents the means of 3-5 independent experiments with 6 replicate samples for each condition. The circle denotes untreated Vero-d2EGFP samples intoxicated with ETA only, and the square denotes the addition of grape seed extract along with ETA.

The EGFP signal from untreated Vero-d2EGFP cells was arbitrarily set as the 100% maximal EGFP signal.

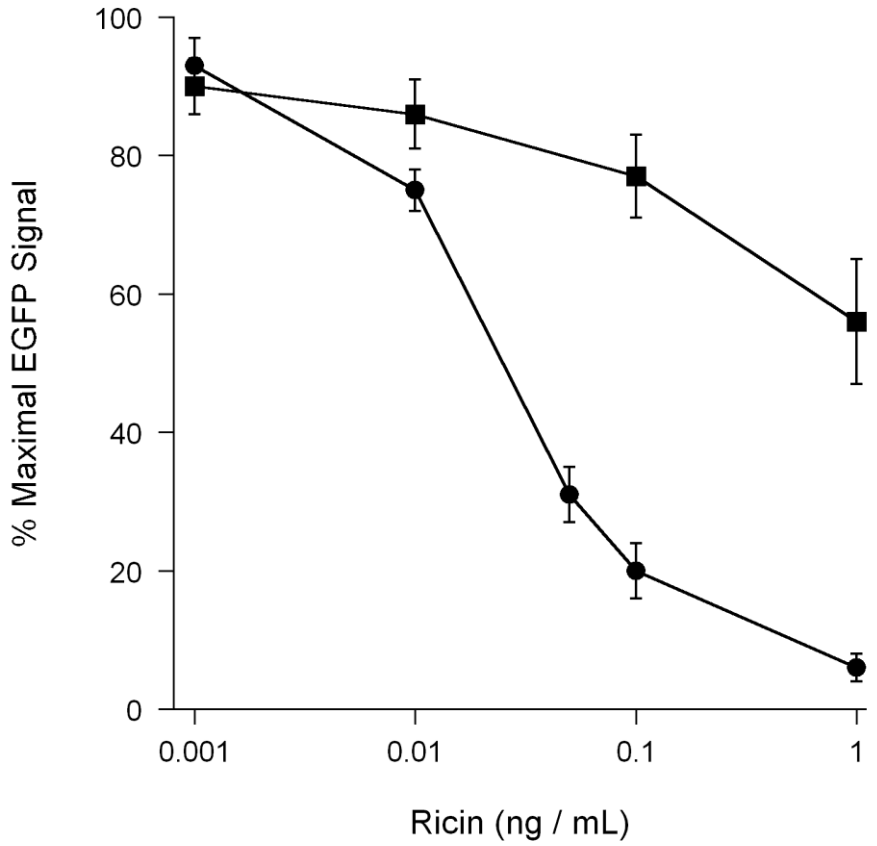

Figure 13: The effect of ricin on Vero-d2EGFP signal.

EGFP signal was measured after an overnight incubation with the indicated concentrations of ricin. Error bar represents the standard errors of the means of 3-5 independent experiments with 6 replicate samples for each condition. The circle denotes untreated Vero-d2EGFP samples intoxicated with ricin only, and the square denotes the addition of grape seed extract.

The EGFP signal from untreated Vero-d2EGFP cells was arbitrarily set as the 100% maximal EGFP signal.

3.2 Phenolic Compounds' Screens against DT, ETA, Ricin, and ST

We demonstrated that the grape seed extract confers resistance against 4 different toxins, namely DT, ETA, ricin, and ST. Since the extract contains substantial quantities of phenolic compounds [82-84], our hypothesis was that these phenolic compounds are responsible for the toxin resistance. Upon advice from Drs. Friedman and Quiñones from the USDA whom are experts in phenolic compound studies, we chose to screen a set of 20 individual phenolic compounds along with the toxins in order to determine the active components of the grape seed extract that are responsible for toxin inhibition. A set of unintoxicated cells and a set of cells treated with 10% glycerol were used as controls. The 10% glycerol solution was used as a positive control. Glycerol is a known protein stabilizer that prevents unfolding of the toxins' catalytic domain that is required for translocation to the cytosol [48, 81].

To monitor the anti-DT property of the individual phenolic compounds, a 0.1 ng/ml concentration of DT was used to intoxicate the cells. When cells were treated with 0.1 ng/ml DT alone, the EGFP signal was lowered to 17 ± 2%. Three of the individual compounds screened, epigallocathechin gallate, caftaric acid, and procyanidin B1, lowered the activity of DT and consequently maintained elevated EGFP signals of 59 ± 3%, 46 ± 9%, and 46 ± 9% of the unintoxicated control value, respectively (Table 2). To monitor the anti-ETA property of the individual phenolic compounds, a 100 ng/ml concentration of ETA was used to intoxicate the Vero-d2EGFP cells. Four of the 20 compounds screened, epicatechin gallate, epigallocathechin gallate, procyanidin B2, and resveratrol showed elevated EGFP signals of 73 ± 12%, 89 ± 10%, 84 ± 13%, and 46 ± 5% of the unintoxicated control value, respectively. This was compared to 22 ± 4% of the control EGFP signal obtained from Vero-d2EGFP cells intoxicated with ETA in the absence of phenolic compounds (Table 2). We then screened the 20 individual phenolic compounds to

determine which ones confer resistance against ricin. To monitor the anti-ricin property of the individual phenolic compounds, a 1 ng/ml concentration of ricin was used to intoxicate the Vero-d2EGFP cells. Only one of the compounds screened, epigallocathechin gallate, showed protection against the activity of ricin with an EGFP signal of 51 ± 10% compared to 19 ± 2% for untreated, ricin-intoxicated Vero-d2EGFP cells (Table 2). Our data show that epigallocathechin gallate confers resistance against multiple toxins, whereas epicatechin gallate, caftaric acid, procyanidin B1, procyanidin B2, and resveratrol affect only one toxin. This observation suggests that the effectiveness of the extract stems from the fact that it contains many different compounds, each affecting one or more toxins.

No individual compound conferred resistance against ST. However, a cocktail of all 20 compounds conferred resistance against ST with an EGFP signal of 52 ± 4% compared to 32 ± 2% for untreated, ST-intoxicated Vero-d2EGFP cells (Table 2). This suggests that two or more compounds in the extract act synergistically to inhibit ST.

Table 2: Phenolic compounds screened against ST, ricin, ETA, and DT.
(David Curtis, Chris Britt, Chris Berndt, and Srikar Reddy also contributed to these data).

- Each value represents the mean of at least three independent experiments with 6 or 12 replicate samples for each condition.
- ± denotes standard error of the mean (SEM).
- Red denotes statistical significance ($p<0.01$, student's t test).

		% Control EGFP Signal (Maximal EGFP Signal- no toxin addition)			
Compound (10 µg/ml)	**Molarity (µM)**	**ST**	**Ricin**	**ETA**	**DT**
No Treatment	--	32 ± 2	19 ± 2	22 ± 4	17 ± 2
10% Glycerol	--	**83 ± 9**	**84 ± 4**	**92 ± 4**	**57 ± 7**
Catechin	34	33 ± 7	22 ± 5	22 ± 3	20 ± 3
Catechin gallate	23	39 ± 7	22 ± 5	15 ± 2	19 ± 2
Epicatechin	34	30 ± 4	20 ± 4	16 ± 2	18 ± 4
Epicatechin gallate	23	38 ± 2	17 ± 5	**73 ± 12**	28 ± 4
Epigallocatechin gallate	22	40 ± 3	**51 ± 10**	**89 ± 10**	**59 ± 3**
Caftaric acid	32	28 ± 1	25 ± 6	15 ± 3	**46 ± 9**
Gallic acid	58	27 ± 4	28 ± 6	17 ± 8	33 ± 7
Procyanidin B1	17	25 ± 4	14 ± 2	20 ± 4	**46 ± 9**
Procyanidin B2	17	27 ± 2	16 ± 3	**84 ± 13**	15 ± 4
Quercitrin	22	22 ± 3	15 ± 1	15 ± 3	9 ± 4
Cyanidin	31	30 ± 6	14 ± 2	14 ± 3	13 ± 3
Delphinidin	30	34 ± 6	17 ± 2	15 ± 5	31 ± 7
Kaempferol	35	32 ± 5	15 ± 4	20 ± 6	19 ± 3
Protocatechin	65	29 ± 7	12 ± 3	13 ± 4	8 ± 4
Resveratrol	44	33 ± 8	20 ± 4	**46 ± 5**	10 ± 2
Kuromanin	21	24 ± 3	19 ± 5	9 ± 3	20 ± 1
Malvin	15	29 ± 6	17 ± 3	28 ± 7	14 ± 2
Oenin	19	27 ± 5	15 ± 2	24 ± 5	17 ± 1
Peonidin	20	30 ± 8	18 ± 4	27 ± 7	14 ± 1
Petunidin	20	31 ± 10	17 ± 4	13 ± 1	15 ± 1
20 compound cocktail	--	**52 ± 4**	--	--	--

3.3 Inhibition of CT Activity by Phenolic Compounds

Reddy et al. have found that grape seed extract confers resistance to CT intoxication [80]. We therefore used a cocktail of 20 compounds to confirm that this inhibition is in fact mediated by phenolic compounds. The data show that our cocktail did in fact significantly lower the cAMP response induced by CT to ~20% of the response generated from cells exposed to 100 ng/ml CT in the absence of the cocktail (Figure 14). To identify the individual compounds responsible for CT inhibition, 10 μg/ml of each of the individual compounds was screened for a block of the CT-induced cAMP accumulation. A greater than 50% cAMP reduction in control cAMP levels was set as an arbitrary cut off for toxin inhibition. Twelve of the compounds screened were found to meet this criterion (Table 3). To investigate whether the compounds affect the activity of adenylate cyclase (AC), we screened mixtures of each compound with forskolin, a known AC agonist [86]. One of the compounds, PB2, was found to partially inhibit the activity of AC. This indicated that PB2, but none of the other 11 compounds, could potentially affect CT activity through an indirect effect linked to the inhibition of AC activity. We then investigated other mechanisms by which the 12 compounds could inhibit CT. Different stages in the CT intoxication process, namely binding to the cell surface, unfolding of CTA1, and CTA1 ADP-ribosylation activity, were investigated (Table 3). By monitoring the fluorescence from a FITC-CTB pentamer bound to the surface of Vero cells, two of the compounds, PB2 and EGCG, were found to partially inhibit binding of CT to the cell surface (58 ± 8% and 57 ± 9% of control signal, respectively). Two other compounds, caftaric acid and kaempferol, partially inhibited the ADP-ribosylation activity of CTA1 (45 ± 7% and 53 ± 4% of control signal, respectively) as measured by an in vitro assay for toxin activity. While the grape seed extract itself prevents the unfolding of CTA1, no individual compounds inhibited the unfolding of CTA1 with the thermolysin protease sensitivity assay. A cocktail of the twelve

phenolic inhibitors of CT also failed to prevent the unfolding activity of CTA1 by the same thermolysin assay. As shown by an MTS viability assay, none of the twelve hit compounds affected cell viability (Table 3). DMSO is known to be toxic to cells; therefore 20% DMSO was used as a negative control during each MTS viability assay. Only about 2% of the control signal remained when cells were treated with 20% DMSO (Data not shown).

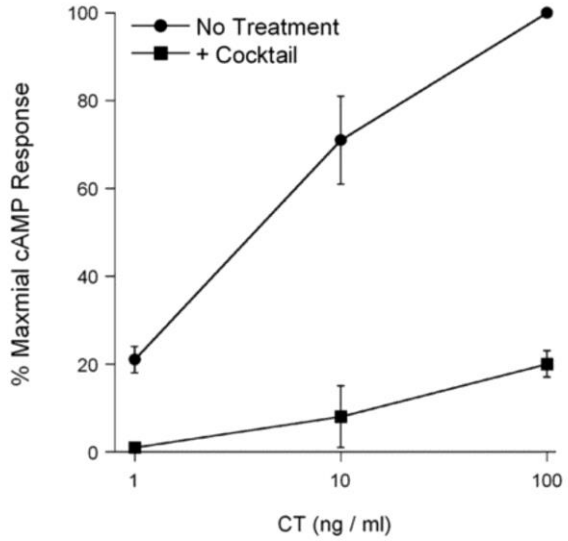

Figure 14: A cocktail of 20 phenolic compounds confers resistance against CT.

- CHO cells were used over a 2 hour incubation period at 37°C under specified conditions. Error bar represents the standard error of the mean of 3 independent experiments with 3 replicate samples for each condition.

Table 3: Phenolic compounds screened against different stages of CT intoxication.
(Camila Garcia also contributed to these data)

- Phenolic compounds screened against in vivo CT activity (cAMP), toxin binding to the cell surface (FITC-CTB), and in vitro CTA1 activity (DEA-BAG).
- Potential toxicity of each compound was screened with an MTS viability assay.
- The % control signal in each assay was arbitrarily set at the 100% value. For cAMP, this value represents the amount of cAMP produced in CHO cells when treated with 100 ng/ml of CT over a 2 hour incubation period at 37°C. For viability, this value represents the absorbance at 490 nm when MTS reagent is added to untreated CHO cells. For FITC-CTB, this value represents the fluorescence signal of FITC-CTB when Vero cells are treated with 1 µg/ml of FITC-CTB for 30 minutes at 4°C. For DEA-BAG, this value represents the fluorescence signal of DEA-BAG at 25°C with 1µg/ml of CTA1 for 2 hours.
- ± denotes the standard error of the mean (SEM) of at least 2 independent experiments or the standard deviation of the number of replicate samples of a single experiment. For cAMP it represents the SEM of at least 2 independent experiments with 3 replicate samples or the SD of 3 replicate samples of 1 experiment. For MTS viability, FITC-CTB, and DEA-BAG, it represents the SEM of at least 3 independent experiments with 6 or 12 replicate samples.
- Bold value represents compounds with anti-CT property.

		% Control Signal			
Compound (10 µg/ml)	**Molarity (µM)**	**cAMP**	**Viability**	**FITC-CTB**	**DEA-BAG**
Catechin	34	98 ± 4	--	--	--
Oenin chloride	19	86 ± 11	--	--	--
Malvin chloride	15	74 ± 18	--	--	--
Epicatechin gallate	23	74 ± 11	--	--	--
Peonidin	20	73 ± 3	--	--	--
Protocatechin	65	72 ± 4	--	--	--
Epicatechin	34	67 ± 14	--	--	--
Catechin gallate	23	63 ± 8	--	--	--
Petunidin	20	**44 ± 2**	100 ± 4	94 ± 4	65 ± 5
Quercitrin	22	**41 ± 8**	97 ± 3	80 ± 5	78 ± 8
Caftaric acid	32	**39 ± 9**	103 ± 2	83 ± 7	**45 ± 7**
Kaempferol	35	**35 ± 9**	117 ± 2	78 ± 6	**53 ± 4**
Procyanidin B2	17	**31 ± 7**	102 ± 7	**58 ± 8**	99 ± 1
Procyanidin B1	17	**30 ± 3**	94 ± 2	79 ± 8	69 ± 3
Gallic Acid	58	**24 ± 1**	103 ± 7	77 ± 5	107 ± 5
Kuromanin	21	**23 ± 15**	97 ± 4	78 ± 6	102 ± 2--
Resveratrol	44	**22 ± 7**	99 ± 5	89 ± 10	108 ± 3
Delphinidin	30	**15 ± 5**	105 ± 5	69 ± 6	76 ± 10
Cyanidin	31	**10 ± 10**	102 ± 4	79 ± 5	113 ± 13
Epigallocatechin gallate	22	**7 ± 3**	88 ± 4	**57 ± 9**	101 ± 6
Seed extract	--	**23 ± 1**	--	**20 ± 3**	**22 ± 7**

PB2 and EGCG Inhibit FITC-CTB Binding

As previously established by Reddy et al. [80], grape seed extract prevents binding of CT to the cell surface. Therefore, the grape seed extract was used as a positive control for additional CT binding assays. We found that a cocktail of PB2 and EGCG, or a cocktail of the twelve hit compounds (the ones that lowered the control cAMP level below 50%) partially inhibited the binding of FITC-CTB on the surface of Vero cells in a dose-dependent manner (Figure 15A). At 100 μg/ml, 10 μg/ml, and 1 μg/ml, the twelve compound cocktail inhibited binding of CT to the cell surface by 37 ± 2%, 64 ± 8%, and 86 ± 2% of the control signal, respectively. At 17, 1.7, and 0.17 μg/ml, the PB2/EGCG cocktail inhibited binding of CT to the cell surface by 23 ± 9%, 57 ± 6%, and 87 ± 2% of the control signal, respectively. At a concentration of 17 μg/ml, the PB2/EGCG cocktail was found to be as effective as 100 μg/ml of the seed extract at inhibiting FITC-CTB binding. The molar amounts of PB2 and EGCG used in both the two compound and the twelve compound cocktails are equivalent, and yet the EGCG/PB2 cocktail exhibits the same potency as the twelve hit compound cocktail. Therefore, it appears nothing else in the twelve compounds cocktail other than PB2 and EGCG is contributing to the inhibition of FITC-CTB binding.

Reddy et al. also established that grape seed extract can strip bound CT off the cell surface [80]. To investigate whether PB2 and EGCG alone or in a cocktail could strip bound FITC-CTB from the cell surface, they were added 30 minutes after FITC-CTB had been bound to the cell surface. The binding of FITC-CTB to the cell surface is conducted at 4°C to avoid the internalization of the bound FITC-CTB. A cocktail made with the twelve hit compounds was also investigated to see if it could strip bound FITC-CTB off the cell surface. These cocktails and individual compounds did in fact strip bound CT off the cell surface (Figure 15B).

To investigate the affinity of the grape seed extract and the two compounds for FITC-CTB, we did a dialysis experiment. A 3.5 kD molecular weight cut off dialysis tube was used to dialyze FITC-CTB overnight in the presence or absence of treatments. With a strong affinity for the FITC-CTB, the grape seed extract and compounds would have remained bound to the toxin and still confer resistance after dialysis. Unlike the seed extract that exhibited a high affinity interaction with FITC-CTB that allowed it to be retained after overnight dialysis, both PB2 and EGCG did not show this high affinity (Figure 15C). After the overnight dialysis, PB2 and EGCG showed a weaker inhibition. This is due perhaps to the loss of some of the compounds after the dialysis. The extract, on the other hand, gets slightly more effective after dialysis. This is perhaps due to the removal of one or more compounds that inhibit the anti-toxin compounds. Since both PB2 and EGCG lost most of their effects after the dialysis, there must be other anti-toxin compound(s) in the extract that were not investigated during the course of this project.

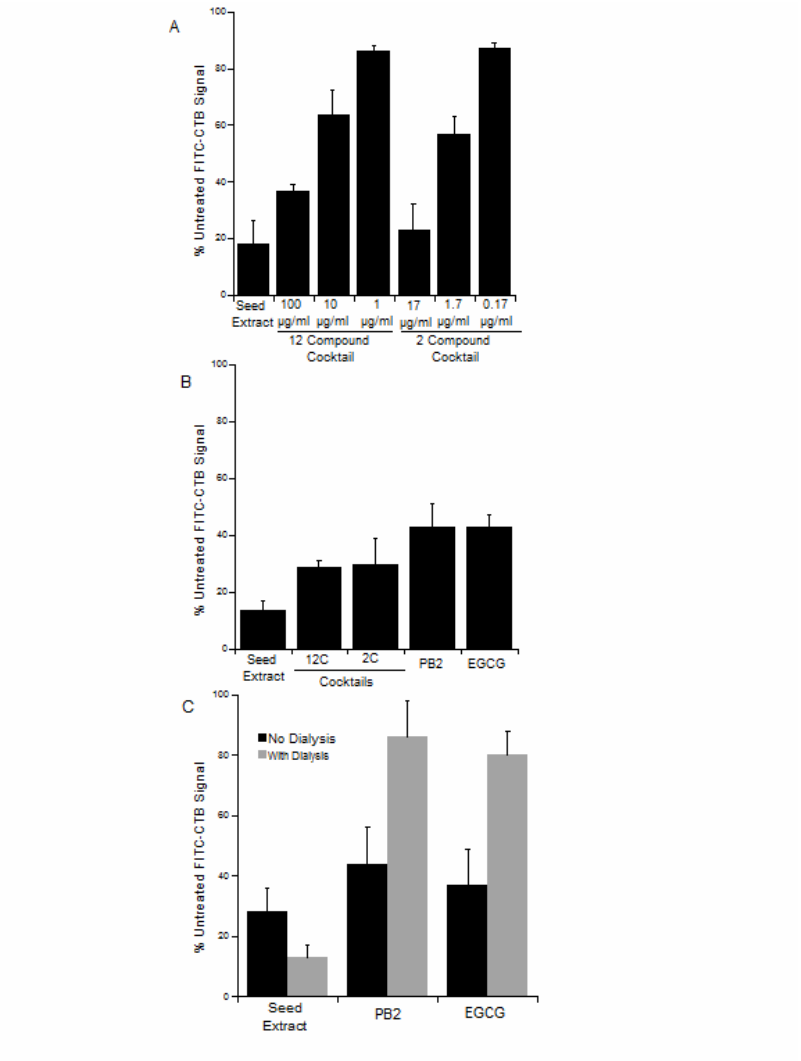

Figure 15: Toxin binding experiments.

Toxin binding to Vero cells in the presence of grape extract, a cocktail of 12 phenolic compounds, a cocktail of 2 phenolic compounds, and two individual compounds. A) The FITC-CTB subunit was co-incubated with the phenolic compounds and seed extract, then applied to Vero cells for 1 hour at 4°C, a temperature that allows toxin binding to the cell surface but prevents toxin endocytosis. B) Addition of seed extract (100 µg/ml), 12 compound cocktail (100 µg/ml),or 2 compound cocktail (17 µg/ml) for 1 hour at 4°C after a 30 minutes 4°C incubation of FITC-CTB and Vero cells. C) Dialysis experiment showing that one or more compounds in the seed extract (100 µg/ml) exhibits a high affinity interaction with the CTB subunit that allows the seed compound(s) to be retained after overnight dialysis. Neither PB2 (10 µg/ml) nor EGCG (10 µg/ml) showed this high affinity with CTB.

Error bar represents the standard error of the mean (SEM) of at least 3 independent experiments with 6 or 12 replicate samples for each condition.

The FITC-CTB signal from cells incubated with FITC-CTB in the absence of phenolic compounds was set as the 100% value.

No Individual Compounds or Cocktails Inhibit the Thermal Unfolding of CTA1

The free CTA1 subunit needs to unfold in order to leave the ER and reach its target in the cytosol. To monitor this unfolding event, the thermolysin protease sensitivity assay was used. As previously established [80], grape seed extract prevented the thermal unfolding of CTA1 (Figure 16A). However, none of the individual compounds or cocktails that we screened were found to inhibit the unfolding of CTA1 (Figure 16A and data not shown). Thus, another compound (or compounds) in the extract must be responsible for the inhibition of CTA1 unfolding. Further experiments confirmed the extract-induced inhibition of CTA1 unfolding was not due to an inhibition of the thermolysin protease itself. For this control experiment, the milk protein α-casein was used, mainly because it has relatively little secondary structure and will always be degraded in the presence of an active protease. Our results confirm that the grape seed extract does not interfere with the thermolysin protease activity (Figure 16B), as the presence of grape extract did not inhibit the proteolysis of α-casein.

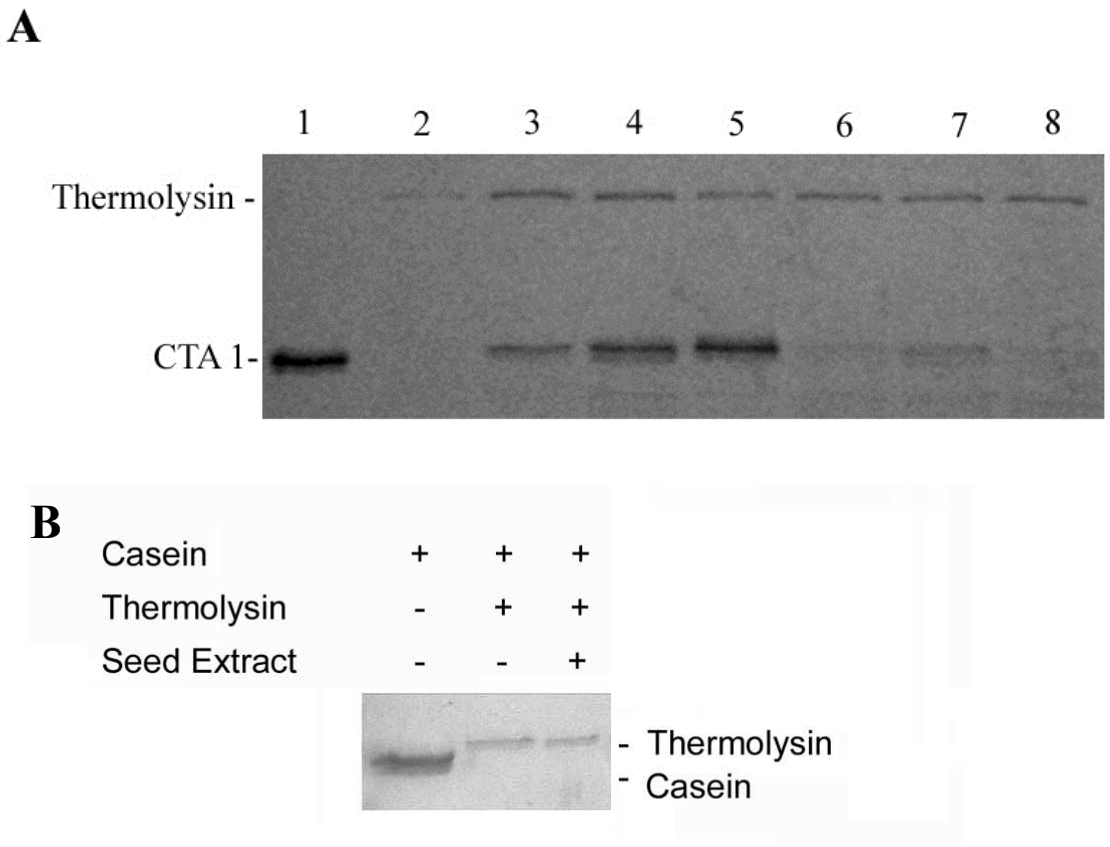

Figure 16: Thermal unfolding of CTA1 at 37°C.

A) The grape seed extract inhibits the thermal unfolding of CTA1, but no individual compounds or cocktails screened inhibit unfolding of CTA1.

1: CTA1 only
2: Thermolysin only
3: Disulfide-linked CTA1/CTA2 heterodimer, which also prevents CTA1 unfolding
4: + 100 µg/ml grape seed extract
5: + 1000 µg/ml grape seed extract
6: + 11 compound cocktail (Quercitrin, Caftaric acid, Kaempferol, PB2, PB1, Gallic Acid, Kuromanin, Resveratrol, Delphinidin, Cyanidin, EGCG) at 100 µg/ml
7: + PB2 (10 µg/ml)
8: + EGCG (10 µg/ml)

Although results for only two individual compounds are shown, none of the individual twelve hit compounds prevented the thermal unfolding and proteolysis of CTA1.

B) The grape seed-induced inhibition of CTA1 unfolding is not due to an inhibition of the thermolysin protease.

CHAPTER 4: DISCUSSION

The present work has evaluated the use of grape seed extract as an anti-toxin agent against cholera and other toxin-mediated diseases. Other plant extracts, including unripe fruit of *Aegle marmelos*, have also been shown to possess antibacterial properties [12, 80]. The grape seed extract used in our study is sold as a nutritional supplement and is generally regarded safe by the United States Food and Drug Administration [87, 88]. In the present work we identified individual phenolic compounds of the grape seed extract that inhibit CT activity, and we also determined some of their mechanisms of action. We also provide evidence that individual phenolic compounds from the grape seed extract contribute to broad-spectrum toxin inhibition against ST, ricin, ETA, and DT. This work provides a foundation for the synthesis of broad-spectrum therapeutic drugs against cholera and other toxin-mediated diseases.

None of the individual compounds screened against ST was found to be inhibitory to its activity. However, a cocktail made of all 20 compounds was found to partially inhibit the cytotoxic effect of ST. This finding suggests some of the compounds in the grape seed extract might act synergistically to inhibit ST. A single compound, EGCG was found to provide a broad-spectrum resistance against ricin, ETA, DT, and CT. The cellular basis of EGCG-generated resistance to these toxins remains to be established. Furthermore, although EGCG did not confer resistance against Shiga toxin 2 that we used in this study, it has recently been reported that EGCG inhibits the cytotoxicity of Shiga toxin 1, a less potent isoform of Shiga toxin [89].

We identified twelve compounds that block CT. None of these twelve compounds has any significant effect on cell viability. The mechanism by which the twelve compounds block CT was investigated. Two of the compounds inhibited binding of CT, EGCG and PB2. Two other

compounds, caftaric acid and kaempferol, inhibited the enzymatic activity of CT. Our data further showed that grape seed extract has a high binding interaction with FITC-CTB. However, the high binding interaction of the grape seed extract with FITC-CTB could not be replicated with the two individual compounds that inhibited binding of FITC-CTB, PB2 and EGCG. This suggests that there might be more than one compound acting synergistically to provide this effect, or there are other compounds in the extract providing this high affinity interaction that were not screened in this study. As seen in Figure 15C, the seed extract provided a better protection after dialysis as compared to the non-dialyzed seed extract. This finding suggests that the overnight dialysis might have helped remove some of the compounds in the grape seed extract that have a negative effect on the anti-toxin compounds present in the extract. This finding also suggests that a defined cocktail might be better than the extract for therapeutic use, because of the absence of the inhibitors of the anti-toxin compounds.

The seed extract, PB2 and EGCG have the ability to remove bound FITC-CTB off the plasma membrane of the cell. The mechanism of action of this phenomenon still remains to be elucidated, but it again shows the high affinity that the seed extract exhibits for CT. It also suggests that EGCG, PB2, and the seed extract can provide protection even after being exposed to CT. There are potential concerns that certain phenolic compounds can induce protein aggregation [90], but our data suggest that the hit compounds at the 10 µg/ml concentration are specific as anti-toxins. If the anti-toxin compounds were inducing non-specific toxin aggregations, they would aggregate all the toxins that were investigated and inhibit their activities, not just a subset of the toxins. Also, compounds at 10 µg/ml are not toxic to cells as confirmed by MTS cell viability assays.

Unlike the seed extract, no individual compound screened was found to inhibit the unfolding of CTA1, a necessary step that allows the toxin to leave the ER and reach the cytosol. However, our

data do confirm that a subset of the compounds have the ability to block multiple events in the cholera intoxication process. Two compounds interfered with the binding of CT to the cell surface, and two different compounds partially inhibited the ADP-ribosylation activity of CTA1. The finding of compounds that inhibit the enzymatic activity of CTA1 further suggests that these compounds might still be effective after being exposed to CT. Although we identified twelve compounds with anti-CT property, we were only able to determine the mechanism of inhibition of four of them. Because neither of the remaining eight compounds could inhibit FITC-CTB binding, prevented unfolding, or prevented the ADP-ribosylation of DEA-BAG, the mechanism of inhibition of these eight compounds must be independent of CT binding, CTA1 unfolding, and CTA1 enzymatic activity.

Recently, there have been growing interests in studying the health benefits of plant extracts. Recent studies have investigated the beneficial properties of various plant extracts. Hop extract, for example, has been investigated against Alzheimer in mice [91], and it is also commercially available as a dietary supplement [92]. Another study has also investigated the anti-CT property of resveratrol, a phenolic compound present in grape seed extract [93]. The mechanism behind the health benefits of most extracts is unknown. Our work on natural products is unique in that it does not only identify toxin inhibitors; it also investigates potential mechanism of action. We have previously shown that grape seed extract inhibits multiple events in the cholera intoxication process. We have also shown that grape seed extract reduces the CT-induced intestinal fluid accumulation using an in vivo animal model [80]. The present work identified grape seed extract as a broad-spectrum anti-toxin. The broad-spectrum anti-toxin provided by grape seed extract stems from the fact that a majority of the extract is composed of phenolic compounds. Different phenolic compound with anti-toxin property affects different toxin at different step in the toxin intoxication

process. Furthermore, we identified phenolic compounds in grape seed extract with anti-toxin properties for five different toxins. Lastly, we identified how a subset of phenolic compounds inhibits CT.

In conclusion, this work has evaluated the use of grape seed extract as an anti-toxin agent against cholera and other diseases caused by AB toxins. We identified individual phenolic compounds of grape seed extract that inhibit CT activity, and we determined some of their mechanisms of action. We have also provided evidence that individual phenolic compounds from grape seed extract contribute to broad-spectrum toxin inhibition against ST, ricin, ETA, and DT. This present work provides a foundation for the synthesis of broad-spectrum therapeutic drugs against cholera and other toxin-mediated diseases.

LIST OF REFERENCES

1. Falnes, P.O. and K. Sandvig, *Penetration of protein toxins into cells.* Curr Opin Cell Biol, 2000. **12**(4): p. 407-13.

2. Choe, S., et al., *The crystal structure of diphtheria toxin.* Nature, 1992. **357**(6375): p. 216-22.

3. Greenfield, L., et al., *Nucleotide sequence of the structural gene for diphtheria toxin carried by corynebacteriophage beta.* Proc Natl Acad Sci U S A, 1983. **80**(22): p. 6853-7.

4. Montecucco, C. and E. Papini, *Cell penetration of bacterial protein toxins.* Trends Microbiol, 1995. **3**(5): p. 165-7; discussion 167-8.

5. Tsuneoka, M., et al., *Evidence for involvement of furin in cleavage and activation of diphtheria toxin.* J Biol Chem, 1993. **268**(35): p. 26461-5.

6. Chiron, M.F., C.M. Fryling, and D.J. FitzGerald, *Cleavage of pseudomonas exotoxin and diphtheria toxin by a furin-like enzyme prepared from beef liver.* J Biol Chem, 1994. **269**(27): p. 18167-76.

7. Donovan, J.J., et al., *Diphtheria toxin forms transmembrane channels in planar lipid bilayers.* Proc Natl Acad Sci U S A, 1981. **78**(1): p. 172-6.

8. Kagan, B.L., A. Finkelstein, and M. Colombini, *Diphtheria toxin fragment forms large pores in phospholipid bilayer membranes.* Proc Natl Acad Sci U S A, 1981. **78**(8): p. 4950-4.

9. Lemichez, E., et al., *Membrane translocation of diphtheria toxin fragment A exploits early to late endosome trafficking machinery.* Mol Microbiol, 1997. **23**(3): p. 445-57.

10. Deng, Q. and J.T. Barbieri, *Molecular mechanisms of the cytotoxicity of ADP-ribosylating toxins.* Annu Rev Microbiol, 2008. **62**: p. 271-88.

11. Morimoto, H. and B. Bonavida, *Diphtheria toxin- and Pseudomonas A toxin-mediated apoptosis. ADP ribosylation of elongation factor-2 is required for DNA fragmentation and cell lysis and synergy with tumor necrosis factor-alpha.* J Immunol, 1992. **149**(6): p. 2089-94.

12. Brijesh, S., et al., *Studies on the antidiarrhoeal activity of Aegle marmelos unripe fruit: validating its traditional usage.* BMC Complement Altern Med, 2009. **9**: p. 47.

13. Hwang, J., et al., *Functional domains of Pseudomonas exotoxin identified by deletion analysis of the gene expressed in E. coli.* Cell, 1987. **48**(1): p. 129-36.

14. Siegall, C.B., et al., *Functional analysis of domains II, Ib, and III of Pseudomonas exotoxin.* J Biol Chem, 1989. **264**(24): p. 14256-61.

15. Allured, V.S., et al., *Structure of exotoxin A of Pseudomonas aeruginosa at 3.0-Angstrom resolution.* Proc Natl Acad Sci U S A, 1986. **83**(5): p. 1320-4.

16. Chaudhary, V.K., et al., *Pseudomonas exotoxin contains a specific sequence at the carboxyl terminus that is required for cytotoxicity.* Proc Natl Acad Sci U S A, 1990. **87**(1): p. 308-12.

17. Hessler, J.L. and R.J. Kreitman, *An early step in Pseudomonas exotoxin action is removal of the terminal lysine residue, which allows binding to the KDEL receptor.* Biochemistry, 1997. **36**(47): p. 14577-82.

18. Kounnas, M.Z., et al., *The alpha 2-macroglobulin receptor/low density lipoprotein receptor-related protein binds and internalizes Pseudomonas exotoxin A.* J Biol Chem, 1992. **267**(18): p. 12420-3.

19. Morris, R.E., M.D. Manhart, and C.B. Saelinger, *Receptor-mediated entry of Pseudomonas toxin: methylamine blocks clustering step.* Infect Immun, 1983. **40**(2): p. 806-11.

20. Fryling, C., M. Ogata, and D. FitzGerald, *Characterization of a cellular protease that cleaves Pseudomonas exotoxin.* Infect Immun, 1992. **60**(2): p. 497-502.

21. Ogata, M., et al., *Cell-mediated cleavage of Pseudomonas exotoxin between Arg279 and Gly280 generates the enzymatically active fragment which translocates to the cytosol.* J Biol Chem, 1992. **267**(35): p. 25396-401.

22. Smith, D.C., et al., *Internalized Pseudomonas exotoxin A can exploit multiple pathways to reach the endoplasmic reticulum.* Traffic, 2006. **7**(4): p. 379-93.

23. Lombardi, D., et al., *Rab9 functions in transport between late endosomes and the trans Golgi network.* EMBO J, 1993. **12**(2): p. 677-82.

24. McKee, M.L. and D.J. FitzGerald, *Reduction of furin-nicked Pseudomonas exotoxin A: an unfolding story.* Biochemistry, 1999. **38**(50): p. 16507-13.

25. Jackson, M.E., et al., *The KDEL retrieval system is exploited by Pseudomonas exotoxin A, but not by Shiga-like toxin-1, during retrograde transport from the Golgi complex to the endoplasmic reticulum.* J Cell Sci, 1999. **112 (Pt 4)**: p. 467-75.

26. Kreitman, R.J. and I. Pastan, *Importance of the glutamate residue of KDEL in increasing the cytotoxicity of Pseudomonas exotoxin derivatives and for increased binding to the KDEL receptor.* Biochem J, 1995. **307 (Pt 1)**: p. 29-37.

27. Iglewski, B.H. and D. Kabat, *NAD-dependent inhibition of protein synthesis by Pseudomonas aeruginosa toxin.* Proc Natl Acad Sci U S A, 1975. **72**(6): p. 2284-8.

28. Irvin, J.D., *Pokeweed antiviral protein.* Pharmacol Ther, 1983. **21**(3): p. 371-87.

29. Vivanco, J.M., B.J. Savary, and H.E. Flores, *Characterization of two novel type I ribosome-inactivating proteins from the storage roots of the andean crop Mirabilis expansa.* Plant Physiol, 1999. **119**(4): p. 1447-56.

30. Christopher, G.W., et al., *Biological warfare. A historical perspective.* JAMA, 1997. **278**(5): p. 412-7.

31. Reisler, R.B. and L.A. Smith, *The need for continued development of ricin countermeasures.* Adv Prev Med, 2012. **2012**: p. 149737.

32. Wolfe, D.N., W. Florence, and P. Bryant, *Current biodefense vaccine programs and challenges.* Hum Vaccin Immunother, 2013. **9**(7): p. 1591-7.

33. Houston, L.L. and T.P. Dooley, *Binding of two molecules of 4-methylumbelliferyl galactose or 4-methylumbelliferyl N-acetylgalactosamine to the B chains of ricin and Ricinus communis agglutinin and to purified ricin B chain.* J Biol Chem, 1982. **257**(8): p. 4147-51.

34. Baenziger, J.U. and D. Fiete, *Structural determinants of Ricinus communis agglutinin and toxin specificity for oligosaccharides.* J Biol Chem, 1979. **254**(19): p. 9795-9.

35. Spooner, R.A., et al., *Protein disulphide-isomerase reduces ricin to its A and B chains in the endoplasmic reticulum.* Biochem J, 2004. **383**(Pt 2): p. 285-93.

36. van Deurs, B., et al., *Routing of internalized ricin and ricin conjugates to the Golgi complex.* J Cell Biol, 1986. **102**(1): p. 37-47.

37. Lord, J.M. and R.A. Spooner, *Ricin trafficking in plant and mammalian cells.* Toxins (Basel), 2011. **3**(7): p. 787-801.

38. Rapak, A., P.O. Falnes, and S. Olsnes, *Retrograde transport of mutant ricin to the endoplasmic reticulum with subsequent translocation to cytosol.* Proc Natl Acad Sci U S A, 1997. **94**(8): p. 3783-8.

39. Sandvig, K. and B. van Deurs, *Endocytosis and intracellular transport of ricin: recent discoveries.* FEBS Lett, 1999. **452**(1-2): p. 67-70.

40. Griffiths, G.D., M.D. Leek, and D.J. Gee, *The toxic plant proteins ricin and abrin induce apoptotic changes in mammalian lymphoid tissues and intestine.* J Pathol, 1987. **151**(3): p. 221-9.

41. Lugnier, A.A., et al., *Inhibition of in vitro protein synthesis in a rabbit reticulocyte cell-free system by toxic trypsic peptides from ricin.* Biochimie, 1974. **56**(9): p. 1287-9.

42. Brigotti, M., et al., *Effect of alpha-sarcin and ribosome-inactivating proteins on the interaction of elongation factors with ribosomes.* Biochem J, 1989. **257**(3): p. 723-7.

43. Nielsen, K. and R.S. Boston, *RIBOSOME-INACTIVATING PROTEINS: A Plant Perspective.* Annu Rev Plant Physiol Plant Mol Biol, 2001. **52**: p. 785-816.

44. Niyogi, S.K., *Shigellosis.* J Microbiol, 2005. **43**(2): p. 133-43.

45. Shiga, K., *Ueber den Erreger der Dysenterie in Japan.* Vorlaufige Mitteilung Zentralbal Bakteriol Microbiol Hyg., 1898. **29**: p. 599-600.

46. Trofa, A.F., et al., *Dr. Kiyoshi Shiga: discoverer of the dysentery bacillus.* Clin Infect Dis, 1999. **29**(5): p. 1303-6.

47. Sandvig, K., et al., *Pathways followed by ricin and Shiga toxin into cells.* Histochem Cell Biol, 2002. **117**(2): p. 131-41.

48. Sandvig, K., I.H. Madshus, and S. Olsnes, *Dimethyl sulphoxide protects cells against polypeptide toxins and poliovirus.* Biochem J, 1984. **219**(3): p. 935-40.

49. Obrig, T.G., *Escherichia coli Shiga Toxin Mechanisms of Action in Renal Disease.* Toxins (Basel), 2010. **2**(12): p. 2769-2794.

50. Sandvig, K., *Shiga toxins.* Toxicon, 2001. **39**(11): p. 1629-35.

51. Garred, O., et al., *Role of the disulfide bond in Shiga toxin A-chain for toxin entry into cells.* J Biol Chem, 1997. **272**(17): p. 11414-9.

52. Olsnes, S., R. Reisbig, and K. Eiklid, *Subunit structure of Shigella cytotoxin.* J Biol Chem, 1981. **256**(16): p. 8732-8.

53. Paton, J.C. and A.W. Paton, *Pathogenesis and diagnosis of Shiga toxin-producing Escherichia coli infections.* Clin Microbiol Rev, 1998. **11**(3): p. 450-79.

54. Garred, O., B. van Deurs, and K. Sandvig, *Furin-induced cleavage and activation of Shiga toxin.* J Biol Chem, 1995. **270**(18): p. 10817-21.

55. Lindberg, A.A., et al., *Identification of the carbohydrate receptor for Shiga toxin produced by Shigella dysenteriae type 1.* J Biol Chem, 1987. **262**(4): p. 1779-85.

56. O'Loughlin, E.V. and R.M. Robins-Browne, *Effect of Shiga toxin and Shiga-like toxins on eukaryotic cells.* Microbes Infect, 2001. **3**(6): p. 493-507.

57. Endo, Y., et al., *Site of action of a Vero toxin (VT2) from Escherichia coli O157:H7 and of Shiga toxin on eukaryotic ribosomes. RNA N-glycosidase activity of the toxins.* Eur J Biochem, 1988. **171**(1-2): p. 45-50.

58. Obrig, T.G., T.P. Moran, and J.E. Brown, *The mode of action of Shiga toxin on peptide elongation of eukaryotic protein synthesis.* Biochem J, 1987. **244**(2): p. 287-94.

59. Chin, C.S., et al., *The origin of the Haitian cholera outbreak strain.* N Engl J Med, 2011. **364**(1): p. 33-42.

60. Spangler, B.D., *Structure and function of cholera toxin and the related Escherichia coli heat-labile enterotoxin.* Microbiol Rev, 1992. **56**(4): p. 622-47.

61. Sack, D.A., et al., *Cholera.* The Lancet, 2004. **363**(9404): p. 223-233.

62. De Haan, L. and T.R. Hirst, *Cholera toxin: a paradigm for multi-functional engagement of cellular mechanisms (Review).* Mol Membr Biol, 2004. **21**(2): p. 77-92.

63. Schafer, D.E., et al., *Elevated concentration of adenosine 3':5'-cyclic monophosphate in intestinal mucosa after treatment with cholera toxin.* Proc Natl Acad Sci U S A, 1970. **67**(2): p. 851-6.

64. Moss, J. and M. Vaughan, *Molecules in the ARF orbit.* J Biol Chem, 1998. **273**(34): p. 21431-4.

65. Majoul, I., D. Ferrari, and H.-D. Söling, *Reduction of protein disulfide bonds in an oxidizing environment.* FEBS Letters, 1997. **401**(2-3): p. 104-108.

66. Orlandi, P.A., *Protein-disulfide isomerase-mediated reduction of the A subunit of cholera toxin in a human intestinal cell line.* J Biol Chem, 1997. **272**(7): p. 4591-9.

67. Taylor, M., et al., *Protein-disulfide isomerase displaces the cholera toxin A1 subunit from the holotoxin without unfolding the A1 subunit.* J Biol Chem, 2011. **286**(25): p. 22090-100.

68. Tsai, B., et al., *Protein disulfide isomerase acts as a redox-dependent chaperone to unfold cholera toxin.* Cell, 2001. **104**(6): p. 937-48.

69. Banerjee, T., et al., *Contribution of subdomain structure to the thermal stability of the cholera toxin A1 subunit.* Biochemistry, 2010. **49**(41): p. 8839-46.

70. Massey, S., et al., *Stabilization of the tertiary structure of the cholera toxin A1 subunit inhibits toxin dislocation and cellular intoxication.* J Mol Biol, 2009. **393**(5): p. 1083-96.

71. Pande, A.H., et al., *Conformational instability of the cholera toxin A1 polypeptide.* J Mol Biol, 2007. **374**(4): p. 1114-28.

72. Taylor, M., et al., *A therapeutic chemical chaperone inhibits cholera intoxication and unfolding/translocation of the cholera toxin A1 subunit.* PLoS One, 2011. **6**(4): p. e18825.

73. Cheng, S.H., et al., *Phosphorylation of the R domain by cAMP-dependent protein kinase regulates the CFTR chloride channel.* Cell, 1991. **66**(5): p. 1027-36.

74. Denning, G.M., et al., *Localization of cystic fibrosis transmembrane conductance regulator in chloride secretory epithelia.* J Clin Invest, 1992. **89**(1): p. 339-49.

75. Field, M., et al., *Effect of cholera enterotoxin on ion transport across isolated ileal mucosa.* J Clin Invest, 1972. **51**(4): p. 796-804.

76. Morinaga, N., et al., *Differential activities of plant polyphenols on the binding and internalization of cholera toxin in vero cells.* J Biol Chem, 2005. **280**(24): p. 23303-9.

77. Oi, H., et al., *Identification in traditional herbal medications and confirmation by synthesis of factors that inhibit cholera toxin-induced fluid accumulation.* Proc Natl Acad Sci U S A, 2002. **99**(5): p. 3042-6.

78. Shrikhande, A.J., *Wine by-products with health benefits.* Food Res. Internat, 2000. **33**(6): p. 469–474.

79. Xia, E.Q., et al., *Biological activities of polyphenols from grapes.* Int J Mol Sci, 2010. **11**(2): p. 622-46.

80. Reddy, S., et al., *Grape extracts inhibit multiple events in the cell biology of cholera intoxication.* PLoS One, 2013. **8**(9): p. e73390.

81. Quinones, B., et al., *Novel cell-based method to detect Shiga toxin 2 from Escherichia coli O157:H7 and inhibitors of toxin activity.* Appl Environ Microbiol, 2009. **75**(5): p. 1410-6.

82. Hernandez-Jimenez, A., et al., *Grape skin and seed proanthocyanidins from Monastrell x Syrah grapes.* J Agric Food Chem, 2009. **57**(22): p. 10798-803.

83. Pastrana-Bonilla, E., et al., *Phenolic content and antioxidant capacity of muscadine grapes.* J Agric Food Chem, 2003. **51**(18): p. 5497-503.

84. Sandhu, A.K. and L. Gu, *Antioxidant capacity, phenolic content, and profiling of phenolic compounds in the seeds, skin, and pulp of Vitis rotundifolia (Muscadine Grapes) As determined by HPLC-DAD-ESI-MS(n).* J Agric Food Chem, 2010. **58**(8): p. 4681-92.

85. Soman, G., et al., *Use of substituted (benzylidineamino)guanidines in the study of guanidino group specific ADP-ribosyltransferase.* Biochemistry, 1986. **25**(14): p. 4113-9.

86. Seamon, K.B., W. Padgett, and J.W. Daly, *Forskolin: unique diterpene activator of adenylate cyclase in membranes and in intact cells.* Proc Natl Acad Sci U S A, 1981. **78**(6): p. 3363-7.

87. Sivaprakasapillai, B., et al., *Effect of grape seed extract on blood pressure in subjects with the metabolic syndrome.* Metabolism, 2009. **58**(12): p. 1743-6.

88. Vinson, J.A., J. Proch, and P. Bose, *MegaNatural((R)) Gold Grapeseed Extract: In Vitro Antioxidant and In Vivo Human Supplementation Studies.* J Med Food, 2001. **4**(1): p. 17-26.

89. Miyamoto T. et al., *Specific inhibition of cytotoxicity of Shiga-like toxin 1 of enterohemorrhagic Escherichia coli by gallocatechin gallate and epigallocatechin gallate.* Elsevier, 2014. **42**.

90. Verhelst, R., et al., *E. coli heat labile toxin (LT) inactivation by specific polyphenols is aggregation dependent.* Vet Microbiol, 2013. **163**(3-4): p. 319-24.

91. Sasaoka, N., et al., *Long-term oral administration of hop flower extracts mitigates Alzheimer phenotypes in mice.* PLoS One, 2014. **9**(1): p. e87185.

92. Krause, E., et al., *Biological and chemical standardization of a hop (Humulus lupulus) botanical dietary supplement.* Biomed Chromatogr, 2014. **28**(6): p. 729-34.

93. Morinaga, N., K. Yahiro, and M. Noda, *Resveratrol, a natural polyphenolic compound, inhibits cholera toxin-induced cyclic AMP accumulation in Vero cells.* Toxicon, 2010. **56**(1): p. 29-35.